Radiative cooling: A review of fundamentals, materials, applications, and prospects

Bin Zhao, Mingke Hu, Xianze Ao, Nuo Chen, Gang Pei*

Department of Thermal Science and Energy Engineering, University of Science and Technology of China, Hefei 230027, China

HIGHLIGHTS

- A detailed introduction and analysis of radiative cooling was reviewed.
- The mathematical description of radiative cooling was reviewed and discussed.
- The emitters' materials and radiative properties were compiled and analyzed.
- The potential applications of radiative cooling were excavated.
- Several recommendations on radiative cooling were presented.

ARTICLE INFO

ABSTRACT

As a passive, effective, and renewable way of decreasing cooling energy requirements without power input, radiative cooling has attracted considerable attention in the field of energy-saving applications. Historically, radiative cooling was limited at nighttime because radiators with strong thermal radiation lack high reflectivity in the solar radiation band. With the recent technological advancements in radiators, such as the development of photonic radiators and metamaterials, the advantages of diurnal radiative cooling has been demonstrated. In this paper, the current state of the art in passive radiative cooling technology is reviewed and updated. First, the fundamental principles of radiative cooling, which comprise different mathematical and physical descriptions, are introduced. Then, the advanced materials and structures of various radiators, which are popular topics in radiative cooling, are presented. Furthermore, application developments in radiative cooling are also summarized and its prospects are preliminarily analyzed. This study provides a detailed introduction and analysis of radiative cooling technology, thereby serving as a key reference for promoting the development of radiative cooling utilization.

1. Introduction

Thermal radiation fundamentally arises from random energy level transitions in matter, indicating that any object at finite temperature can intrinsically achieve thermal emission of energy [1,2]. Thus, radiative heat transfer is one of the most commonly used natural methods of energy transport. The universe, at a temperature close to absolute zero, represents a substantial renewable thermodynamic resource and simultaneously behaves as an ultimate heat sink. Thus, terrestrial objects can dissipate heat into outer space in the form of electromagnetic waves via radiative cooling. The novelty of radiative cooling lies in its ability to achieve cooling without any extra input energy. This passive cooling mechanism has the potential to dissipate excess heat from the earth to the universe, especially in the coming decades, with the

increasing likelihood of extreme heatwaves as a result of climate change [3].

The sky atmosphere, which exists between the earth surface and the universe, is a complex mixture of numerous gases (e.g., oxygen and nitrogen) [4,5] that act as semi-transparent media for radiative cooling. From the radiative property viewpoint, the atmosphere weakens the thermal radiation from the earth surface to the universe in the majority of wavelength bands due to its low transmittance. However, in the wavelength range of 8–13 μm (atmospheric window), the atmosphere is highly transparent for thermal radiation [6]. This atmospheric window coincides with the peak wavelength of thermal radiation from terrestrial objects at a typical ambient temperature. Thus, any sky-faced terrestrial object with high emissivity in the atmospheric window can radiate heat to outer space. The transmittance of atmospheric window

---

is affected by many factors, such as geographical location [7], cloud coverage [8,9], and humidity conditions [7,10,11]. Normally, if the sky is clear and dry, then the transmittance of atmospheric window is high [12].

In previous studies, the importance of nocturnal radiative cooling and its potential applications were extensively investigated and demonstrated. Two types of typical radiators were applied for efficient nocturnal radiative cooling. First type of radiator is near-black radiator, which exhibits high emissivity at almost all thermal radiation bands. Second type of radiator is selective radiator, which has strong thermal emission only in the atmospheric window. Compared with the selective radiator, the near-black radiator has a relatively higher cooling power at a typical ambient temperature; however, its additional atmospheric radiation absorption outside the atmospheric window limits the allotted minimum temperature for the radiator. Notably, the aforementioned radiators with high emissivity in atmospheric window and/or entire thermal radiation band do not have high reflectivity in the solar radiation band at daytime, thus limiting the application of most of these radiators during daytime.

Fortunately, with the emergence of advanced design and fabrication technologies, new classes of selective infrared radiators, including photonic structures and metamaterials, have been rapidly developed in recent studies. Thus, diurnal radiative cooling well below the ambient temperature has been achieved. These novel radiators exhibit high reflection within a solar radiation band (i.e., 0.3–4.0 μm) while simultaneously strongly emitting within the atmospheric transparent window, offering substantial diurnal radiative cooling. Here, diurnal radiative cooling for sub-ambient phenomenon under direct sunshine was initially experimentally demonstrated by Raman et al. [13] based on a planar photonic radiator. This radiator, which consists of seven alternating layers of hafnium dioxide (HfO_2) and silica (SiO_2) with varying thickness on top of 200 nm thick silver (Ag) and 750 μm thick silicon (Si) wafer substrate, can reflect approximately 97% of incident solar irradiance and simultaneously emit strong thermal radiation.

In recent decades, total energy consumption has gradually increased along with economic progress. Thus, radiative cooling, which can act as a novel strategy to release heat of terrestrial objects and passively obtain cooling energy by radiating heat into the cold sink of outer space, is an appealing concept for energy saving and/or harvesting applications. Thus, summarizing and compiling the detailed information on radiative cooling technology are necessary for application reference. To the knowledge of the authors, several review papers on radiative cooling have been published in energy-related journals. Family et al. [14] provided a brief overview of mainstream materials that includes cermet, paints and coatings, and metal oxides for radiative cooling of buildings. Lu et al. [15] mainly reviewed the advanced progress of passive radiative cooling in buildings, including the development of theoretical models and calculations, configuration of cooling structures and systems, and prediction of potential and prospects. Hossain [7] and Sun [16] introduced the concept of radiative cooling from basic principles, materials, and radiators; the main subject is the progress of advanced materials and radiators, including metamaterials and photonic radiators, for radiative cooling. Vall et al. [17] conducted a detailed summary of the theory and nocturnal radiator of the radiative cooling, especially with regard to atmospheric radiation and selective radiator; several numerical simulation methods and prototypes of radiative cooling were also discussed in the articles. Zeyghami et al. [12] presented an up-to-date status of the radiative cooling technology, mainly focusing on universal theory and selective radiators and the potential use of clear sky radiative cooling in renewable energy power systems. The existing papers focus on various aspects of radiative cooling, including modeling summary, materials review, and building application development. However, the systematic description of radiative cooling which simultaneously includes detailed principles, advanced materials and structures, and abundant applications is limited. Besides, the applications of radiative cooling have been largely and innovatively extended in recent years, whereas these applications have not been summarized and analyzed in above reviews. Motivated by this point, a review paper that contains detailed and systematic mathematical descriptions of radiative cooling, an information update of numerous advance radiators, and an introduction of abundant novel applications of radiative cooling was compiled.

In this paper, the current state of the art relevant to radiative cooling technology is adequately reviewed on the basis of previous literatures, involving fundamental principles, advanced materials and structures, and potential application developments and prospects. In Section 2, the fundamental principles of radiative cooling, which consist of different mathematical and physical descriptions of thermal radiation, infrared sky radiation, solar radiation, and parasitic cooling loss are introduced in detail. Specifically, three classic viewpoints relating to the infrared sky radiation based on different assumptions of atmospheric radiative properties were compared. Besides, the universal-mathematical description of parasitic cooling loss and its physical limitation were particularly discussed. In Section 3, the materials, structures, and optical properties of various radiators, which are the key parameters for achieving radiative cooling and have always been a research hotspot, are presented and analyzed in the order of the types of radiator that include natural radiator, film-based radiator, nanoparticle-based radiator, and photonic radiator. In Section 4, the detailed application developments of radiative cooling are summarized and its prospects are preliminarily analyzed. Three kinds of typical building integrated radiative cooling systems, especially for spectral selective based hybrid system, were compiled for energy-saving buildings. The research and development of radiative cooling for solar cells for photovoltaic technology was also reviewed. Besides, personal thermal management, a novel application of radiative cooling, was also introduced and discussed. Moreover, some potential applications, such as radiative cooling to achieve an ultra-low temperature phenomenon in terrestrial, were also briefly mentioned. At the end of the paper, several important and meaningful conclusions are presented based on the aforementioned analysis, thereby providing a reference for the use of radiative cooling technology.

2. Fundamental principles of radiative cooling

In this section, the fundamental principles of radiative cooling, including various theoretical models and corresponding discussions, are presented. The energy balance process of a radiator in radiative cooling process is illustrated in Fig. 1, where q_{rad} denotes the energy radiated, q_{sun} is the solar energy absorbed, q_{sky} refers to the atmospheric radiative energy absorbed, and q_{loss} represents the intrinsic cooling loss.

According to energy balance theory, the net radiative cooling power of the radiator is the comprehensive manifestation of the four preceding energy flows mentioned and can be expressed as follows [13]:
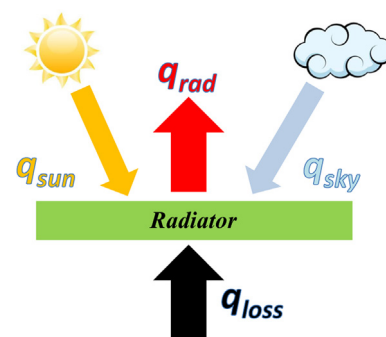

Fig. 1. Energy flows of radiator. q_{sun} is the absorbed solar radiation, q_{sky} is the absorbed atmospheric radiation, q_{rad} is the thermal radiation, and q_{loss} is the intrinsic cooling loss.

Table 1
Summary of correlations of SD–DD sky atmospheric emissivity.

Authors	Year	Correlations	Notes
Granqvist et al. [19]	1981	$\varepsilon_s(\lambda, \theta) = 1 - [1 - \varepsilon_s(\lambda, 0)]^{1/cos(\theta)}$	$\varepsilon_s(\lambda, 0)$ is the emissivity of the atmosphere at vertical direction
Raman et al. [13]	2014	$\varepsilon_s(\lambda, \theta) = 1 - [\tau_s(\lambda, 0)]^{1/cos(\theta)}$	$\tau_s(\lambda, 0)$ is the transmittance of the atmosphere at vertical direction
Zhu et al. [20]	2014		
Bao et al. [21]	2017		
Li et al. [22]	2017		
Lushiku et al. [23]	1982	$\varepsilon_s(\lambda, \theta) = \begin{cases} 1 & (\lambda < 8 \ \mu m, \ \lambda > 13 \ \mu m) \\ 1 - [1 - \varepsilon_s(0)]^{1/cos(\theta)} & (8 \ \mu m < \lambda < 13 \ \mu m) \end{cases}$	$\varepsilon_s(0)$ is average zenith emissivity of the atmosphere
Lushiku et al. [24]	1984		
Berdahl et al. [25]	1983	$\varepsilon_s(\lambda, \theta) = 1 - (1 - \varepsilon_s)[\tau_s(\lambda, 0)/\tau_{average}]e^{1.7b - \frac{1}{cos(\theta)}b}$	ε_s is total atmospheric emissivity; $\tau_{average}$ is average transmittance of the atmosphere; b is an empirical parameter

$$q_{net-cooling} = q_{rad}(T_r) - q_{sky} - q_{sun} - q_{loss} \qquad (1)$$

where $q_{net-cooling}$ is the net radiative cooling power of the radiator, W, and T_r denotes the absolute temperature of the radiator, K. The related theories and calculations of different energy flows expressed in Eq. (1) are summarized and analyzed in the following subsection.

2.1. Thermal radiation fundamentals

The concept of thermal radiation is generally associated with surface and/or volume at a finite temperature. The mechanism of thermal radiation is closely related to energy released due to oscillations and/or transitions of numerous electrons constituting matter [18]. These oscillations are, in turn, sustained by the internal energy of the matter and the temperature. Here, considering a sky-faced radiator (which is assumed to be a surface) of real area A_r at temperature T_r, whose thermal radiation power is defined as q_{rad}, can be calculated by

$$q_{rad}(T_r) = A_r \int_0^{+\infty} \int_0^{2\pi} \int_0^{\pi/2} \varepsilon_r(\lambda, \theta, \varphi, T_r) I_b(\lambda, T_r) cos(\theta) sin(\theta) d\theta d\varphi d\lambda \qquad (2)$$

where $\varepsilon_r(\lambda, \theta, \varphi, T_r)$ denotes the spectral directional emissivity of the radiator at the surface temperature T_r; $I_b(\lambda, T_r)$ is the spectral radiation intensity of a blackbody at temperature T_r, $W \cdot m^{-2} \cdot sr^{-1} \cdot \mu m^{-1}$. In real applications, the effect of azimuth angle on $\varepsilon_r(\lambda, \theta, \varphi, T_r)$ can be neglected for most engineering calculations [18]. Moreover, the effect of surface temperature T_r on $\varepsilon_r(\lambda, \theta, \varphi, T_r)$ can be ignored due to limited temperature variation for radiative cooling [13]. Thus, the expression radiation power of the radiator is simplified as

$$q_{rad}(T_r) = A_r \pi \int_0^{+\infty} \int_0^{\pi/2} \varepsilon_r(\lambda, \theta) I_b(\lambda, T_r) sin(2\theta) d\theta d\lambda \qquad (3)$$

2.2. Infrared sky radiation

The sky atmosphere is a complex mixture of numerous gases (e.g., water vapor and nitrogen) that act as a semi-transparent radiator and weaken the thermal radiation from the earth to the outer space in the majority of wavelength bands. The sky radiation is mainly focused on the infrared wavelength band due to the comprehensive effect of different gases and sky temperatures. However, the sky atmosphere is highly transparent within the atmospheric window (mainly 8–13 μm), which is the key channel for radiative cooling. According to the principles of thermal radiation, the absorbed infrared sky radiation by the radiator can be given by

$$q_{sky} = A_r \pi \int_0^{+\infty} \int_0^{\pi/2} \alpha_r(\lambda, \theta) I_s(\lambda, \theta, T) sin(2\theta) d\theta d\lambda \qquad (4)$$

where $I_s(\lambda, \theta, T)$ denotes the spectral directional radiation power of the sky atmosphere; $\alpha_r(\lambda, \theta)$ is the spectral directional absorptivity of the radiator, which can be replaced by the spectral directional emissivity of the radiator $\varepsilon_r(\lambda, \theta)$ based on Kirchhoff radiation law.

According to previous studies, three classic viewpoints, namely, spectral dependent and directional dependent (SD–DD), spectral independent and directional independent (SI–DI), and spectral dependent but directional independent (SD–DI) methods, have been developed to deal with Eq. (4), which is compiled contrastively in the following section.

2.2.1. Spectral-dependent and directional-dependent (SD–DD) viewpoint

The radiative property of the sky atmosphere is assumed to be spectral- and directional- dependent. Thus, the spectral directional radiation intensity of the sky atmosphere, which is defined as $I_s(\lambda, \theta, T)$ in Eq. (4), can be described as

$$I_s(\lambda, \theta, T) = \varepsilon_s(\lambda, \theta) \cdot I_b(\lambda, T_a) \qquad (5)$$

where $\varepsilon_s(\lambda, \theta)$ denotes the spectral directional emissivity of the sky atmosphere and T_a is the absolute temperature of the ambient surrounding, K.

Evaluating the infrared sky radiation based on the viewpoint of SD–DD is a basic method with reliable accuracy. Owing to the complex effect of different gases on the radiative property of the sky atmosphere and its calculation difficulty in the theoretical model, the related correlations of sky atmospheric emissivity, which are presented in Table 1, are limited.

2.2.2. Spectral-independent and directional-independent (SI–DI) viewpoint

If the infrared sky radiation is handled to be SI–DI, then the description of sky infrared radiation can be simplified and the radiation power can be easily obtained. Based on the first law of thermodynamics, two typical approximations were covered in almost all relevant literature.

First, the sky atmosphere is assumed to be a complete blackbody at an effective sky temperature of T_{s-eff}. Thus, the $I_s(\lambda, \theta, T)$ in Eq. (4) is expressed as follows:

$$I_s(\lambda, \theta, T) = I_b(\lambda, T_{s-eff}) \qquad (6)$$

Second, sky atmosphere is assumed to be an actual body at ambient temperature of T_a, with an effective emissivity of ε_{s-eff}. Thus, the radiative intensity $I_s(\lambda, \theta, T)$ is given by:

$$I_s(\lambda, \theta, T) = \varepsilon_{s-eff} I_b(\lambda, T_a) \qquad (7)$$

According to the first law of thermodynamics, when Eqs. (6) and (7) are combined, the relation between the effective sky temperature and emissivity can be derived as shown in Eq. (8), proving the interdependence of these two effective parameters.

$$T_{s-eff} = (\varepsilon_{s-eff})^{1/4} T_a \qquad (8)$$

The sky radiation data can be measured with specific equipment, such as a conventional pyrgeometer or modified infrared thermometer [26], which provides a considerable amount of sky radiation data for analysis. Historically, correlations regarding the effective of sky temperature and emissivity and the sky radiation itself are abundant,

Table 2

Summary of correlations of SI–DI sky atmospheric emissivity. (*Note:* The symbols √, ×, and − in the column "Sky" represent clear sky, cloudy sky, and average condition, respectively.)

Authors	Year	Sky	Correlations	Notes
Brunt [27]	1932	√	$E_s = (C_1 + C_2 e_a^{1/2})\sigma T_a^4$	1. e_a: water vapor pressure, mb 2. C_1, C_2: empirical coefficients, depends on region
Angstrom [28]	1936	√	$E_s = (C_1 - C_2 10^{-C_3 e_a})\sigma T_a^4$	1. e_a: water vapor pressure, mb 2. C_1-C_3: empirical coefficients, depends on region
Bliss [4]	1961	√	$\varepsilon_{s-eff} = 0.8004 + 0.00396 T_{dp}$	1. T_{dp}: dew point temperature, ˚C 2. Theoretical prediction
Swinbank [29]	1963	√	$E_s = -17.09 + 1.195\sigma T_a^4$	1. Based on measured sky data in Benson and Kerang, and et al.
Swinbank [29]	1963	√	$E_s = 5.31 \times 10^{-14} T_a^6$	1. Based on measured sky data in Benson and Kerang, and et al.
Idso et al. [30]	1969	√	$\varepsilon_{s-eff} = 1 - 0.261 e^{-0.00077(273 - T_a)^2}$	1. Based on the measured sky data in Arizona and Alaska
Staley et al. [31]	1972	√	$\varepsilon_{s-eff} = C_1 e^{C_2}$	1. C_1, C_2: empirical coefficients. At standard atmospheric pressure, $C_1 = 0.67$ and $C_2 = 0.08$
Idso [32]	1981	√	$\varepsilon_{s-eff} = 0.7 + 0.0000595 e_a e^{(1500/T_a)}$	1. T_a: ambient temperature, K 2. e_a: water vapor pressure, mb
Berdahl et al. [33]	1982	√	$\varepsilon_{s-eff} = \begin{cases} 0.741 + 0.0062 T_{dp}, & (night) \\ 0.727 + 0.0060 T_{dp}, & (day) \end{cases}$	1. T_{dp}: dew point temperature, ˚C 2. Based on measured sky data in Tucson, Arizona; Gaithersburg, Maryland; and St. Louis, Missouri
Berdahl et al. [34]	1984	√	$\varepsilon_{s-eff} = 0.711 + 0.0056 T_{dp} + 0.000073 T_{dp}^2$ $+ 0.013 cos(t)$	1. T_{dp}: dew point temperature, ˚C 2. t: solar time, hours 3. Based on measured sky data in six cities, including Tucson and San Antonio; and et al.
Berger et al. [35]	1984	√	$\varepsilon_{s-eff} = 0.770 + 0.0038 T_{dp}$	1. T_{dp}: dew point temperature, ˚C 2. Based on measured sky data in France
Martin et al. [36]	1984	×	$\varepsilon_{s-eff} = \varepsilon_{clear-sky} + (1 - \varepsilon_{clear-sky})F$	1. $\varepsilon_{clear-sky}$: sky emissivity at clear sky conditions 2. F: comprehensive cloud factor
Sugita et al. [9]	1993	×	$E_s = E_{clear-sky}(1 + 0.0496 m^{2.45})$	1. $E_{clear-sky}$: sky radiation at clear sky conditions; m: cloudiness 2. Based on measured sky data in Kansas
Chen et al. [37]	1995	−	$\varepsilon_{s-eff} = 0.736 + 0.00571 T_{dp} + 3.3318 \times 10^{-6} T_{dp}^2$	1. T_{dp}: dew point temperature, ˚C 2. Based on measured sky data in Bennington, Nebraska
Niemela et al. [38]	2001	√	$\varepsilon_{s-eff} = \begin{cases} 0.72 + 0.009(e_a - 2), & (e_a \geqslant 2) \\ 0.72 - 0.076(e_a - 2), & (e_a < 2) \end{cases}$	1. e_a: water vapor pressure, hpa 2. Based on measured sky data in Sodankylä, Finland
Tang et al. [39]	2004	√	$\varepsilon_{s-eff} = 0.754 + 0.0044 T_{dp}, (night)$	1. T_{dp}: dew point temperature, ˚C 2. Limited in Negev Highlands
Lhomme et al. [40]	2007	√	$\varepsilon_{s-eff} = 1.18(e_a/T_a)^{1/7}$	1. e_a: water vapor pressure, hpa
Lhomme et al. [40]	2007	×	$\varepsilon_{s-eff} = \varepsilon_{clear-sky}(1.37 - 0.34s)$	1. s: ratio of solar radiation under cloudy sky to that under clear sky
Sicart et al. [41]	2010	×	$\varepsilon_{s-eff} = C_1(e_a/T_a)^{1/m}F$	1. C_1, m:: empirical coefficients, depends on region 2. e_a: water vapor pressure, hp; F: cloud emission factor

ranging from semi-empirical methods to theoretical/experimental methods. The detailed correlations and corresponding information, such as regional/seasonal applicability, are reviewed and summarized in Table 2.

2.2.3. Spectral-dependent but directional-independent (SD–DI) viewpoint

In this case, the radiative property of the sky atmosphere is spectrally selective. Thus, the $I_s(\lambda, \theta, T)$ in Eq. (4) and the total sky radiation power E_s can be expressed as follows:

$$\begin{cases} I_s(\lambda, \theta, T) = \varepsilon_s(\lambda) I_b(\lambda, T_a) \\ E_s = \int_0^{+\infty} \int_0^{2\pi} \int_0^{\pi/2} \varepsilon_s(\lambda) I_b(\lambda, T_a) sin(\theta) cos(\theta) d\theta d\varphi d\lambda \\ \quad = \pi \int_0^{+\infty} \varepsilon_s(\lambda) I_b(\lambda, T_a) d\lambda \end{cases} \quad (9)$$

Generally, the description and calculation of SD–DI are simpler than those of SD–DD but are more complex than those of SI–DI. However, the literature on SD–DI viewpoint is relatively limited. In 1987, based on the modification of rigorous computation methods for sky radiation, Das et al. [42] developed a spectral-related sky emissivity (Eq. (10)) that uses the precipitable water vapor amount as the only input parameter for any geographic latitude and season.

$$\varepsilon_s(\lambda) = 1 - exp[a(\lambda) + b(\lambda)w + c(\lambda)w^2 + d(\lambda)w^3] \quad (10)$$

where $a(\lambda)$, $b(\lambda)$, $c(\lambda)$, and $d(\lambda)$ are spectral-dependent coefficients; w indicates the water vapor amount, cm; λ and w are limited to (5.25 μm, 42.83 μm) and (0.31 cm, 3.68 cm), respectively.

Inserted in Eq. (10), the precipitable water vapor amount w is the total amount of water vapor in the zenith direction between the ground and the top of the sky atmosphere. The total amount of water vapor is

often described as the thickness of the liquid water that would be generated if all the water vapor in the zenith direction was condensed within a unit cell. The detailed description of the total water vapor amount is mostly represented by empirical formulas. The related information is in reference [43] and is not expanded in this paper.

2.2.4. Brief summary

The SI-DI viewpoint was developed on the assumption that the sky atmosphere is considered to be non-spectral selective. Thus, the effective emissivity and/or sky temperature can be obtained based on the energy balance. Considering the differences of different sky conditions, some meteorological parameters, such as dew point temperature, water vapor pressure and et al., were related to the empirical correlation of the effective emissivity and/or sky temperature, which is a rough estimation of sky infrared radiation. If the spectral property of the atmosphere was considered, the SD-DI approach was produced, which is an improvement for increasing the accuracy of description of sky infrared radiation. Actually, the radiative property of the sky atmosphere is spectral- and directional- dependent; thus, the SD-DD approach of sky infrared radiation is currently the most realistic description, which considers the fact that the sky atmosphere is a semi-transparent media that relate to spectrum and radiation angle. Thus, this method has been recognized as a universal description of sky infrared radiation and widely used in recent research for performance prediction of radiative cooling.

2.3. Solar radiation

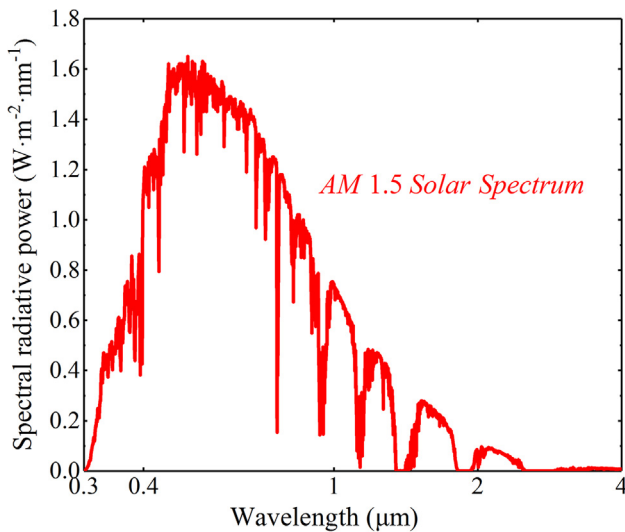The effect of solar radiation is crucial for diurnal radiative cooling.

Fig. 2. Standard AM 1.5 solar spectrum with total solar radiation of approximately 1000 W·m^{-2} [44].

For example, if solar radiation is 800 W·m^{-2}, then the absorbed solar power of a radiator with 5–10% solar absorption is 40–80 W·m^{-2}, approaching or even exceeding the cooling potential of the radiator. The absorbed solar radiation by a radiator, which is defined as q_{sun} in Eq. (1), can generally be expressed as follows [13]:

$$q_{sun} = A_r G \frac{\int_0^{+\infty} \alpha_r(\lambda, \theta_{sun}) I_{AM1.5}(\lambda) d\lambda}{\int_0^{+\infty} I_{AM1.5}(\lambda) d\lambda} \tag{11}$$

where θ_{sun} is the angle where the radiator faces the sun and is assumed to be fixed; $I_{AM1.5}(\lambda)$ denotes the AM 1.5 spectrum distribution of the solar radiation. A standard AM 1.5 spectrum profile [44] (solar radiation = 1000 W·m^{-2}) is shown in Fig. 2 for reference. Notably, the spectral radiative energy can be experimentally tested by solar spectroradiometer. This experimental method can validate the applicability of universal AM 1.5 spectrum for local climate condition.

2.4. Intrinsic cooling loss process

The intrinsic cooling loss of the radiator, including the effect of convection, conduction, and radiation, is a vital variation for the performance estimation of radiative cooling. Specifically, convection and conduction heat transfer are always regarded as the main mechanisms of cooling loss. If the operating temperature of the radiator is higher than the ambient temperature, then the cooling loss power of the radiator is negative, indicating the enlargement of the overall cooling power in this process. However, for sub-ambient radiative cooling, this cooling loss process has a negative influence on minimum temperature which can be potentially reached.

Based on the second law of thermodynamics, sub-ambient cooling phenomenon and/or cooling energy is found to be valuable. Thus, two solutions for sub-ambient radiative cooling were applied to reduce the intrinsic cooling loss power. First, the radiator was encapsulated with specific media (such as air and vacuum [45]) with low thermal conductivity and surrounded by insulation frameworks [46]. Second, the convection shield was used to reduce the cooling loss power of the radiator; for example, low-/high-density polyethylene (L/H-DPE) [13,47], pigmented PE foils [48,49], and zinc selenide (ZnSe) [45] were usually selected as the preferred materials due to their high transmittance within the sky atmospheric window. Moreover, the use of a wind barrier is an alternative method to reduce the cooling loss power of the radiator by separating the ambient airflow from the radiator [50]. In previous studies, infrared-transparent cover is the most popular candidate of convection shield for sub-ambient radiative cooling.

The mathematical description of the intrinsic cooling loss power of the radiator, which is defined as q_{loss} in Eq. (1), can be expressed as follows, relating the radiator and ambient air directly with a comprehensive heat transfer coefficient h:

$$q_{loss} = hA_r(T_a - T_r) \tag{12}$$

If the radiator temperature is higher than the ambient temperature, then the radiator is directly exposed to the ambient air. In this case, the value of h is often determined by empirical formulas, such as the following:

$$h = 2.8 + 3.0u_a \tag{13}$$

where u_a is the velocity of the wind, m·s^{-1}. Eq. (13) is also a universal expression in the performance estimation of solar energy systems [51].

For sub-ambient radiative cooling, the value of h can be calculated from the experimental data. For example, commercial software, including COMSOL, can be applied to simulate the intrinsic cooling loss process of the radiator and determine the value of h. For a specific case [13], the value of h was predicted to be 6.9 W·m^{-2}·K^{-1} based on the energy balance principle. Moreover, the lumped capacitance method is a feasible method to determine the value of h. For example, in Ref. [52], the value of h was predicted to be 10 W·m^{-2}·K^{-1}.

Notably, Eq. (12) is limited for specific occasions. Based on Eq. (12), if $T_a = T_r$, then the effect of the intrinsic cooling loss is thoroughly eliminated. However, in real applications, the intrinsic cooling loss of the radiator is a direct manifestation of the heat transfer between the local surroundings (which includes interface and internal air in the cooling space) and the radiator, and the corresponding illustration is shown in Fig. 3. For example, if the temperature of the cooling space interface is higher than the ambient air temperature, then the intrinsic cooling loss of the radiator occurs even under the assumption of $T_a = T_r$. In actual conditions, the temperature of the cooling space interface is usually higher than the ambient air temperature due to the solar absorption of the cooling space interface.
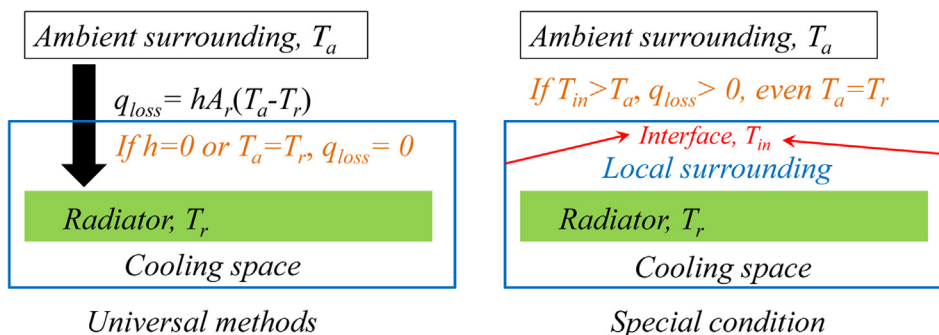

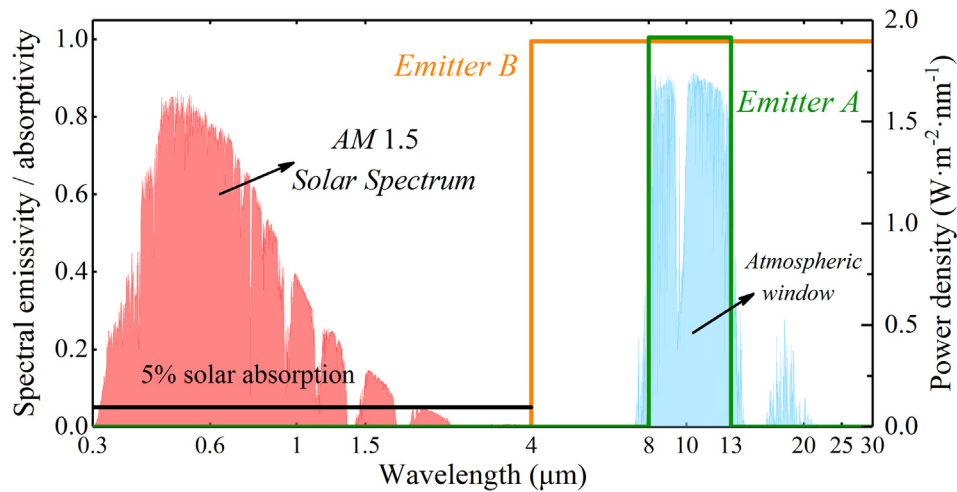**Fig. 3.** Schematic of intrinsic cooling loss process.

Fig. 4. Radiative properties of different radiators, with AM 1.5 solar spectrum and a typical atmospheric window plotted as reference.

2.5. Cooling principle and potential

A widely accepted mathematical model was developed to predict the performance of radiative cooling by combining above main equations, which is shown as follows:

$$
\begin{cases}
q_{net-cooling} = q_{rad}(T_r) - q_{sky} - q_{sun} - q_{loss} \\
q_{rad}(T_r) = \int_0^{+\infty} \int_0^{2\pi} \int_0^{\pi/2} \varepsilon_r(\lambda, \theta, \varphi, T_r) I_b(\lambda, T_r) \cos(\theta) \sin(\theta) d\theta d\varphi d\lambda \\
q_{sky} = \pi \int_0^{+\infty} \int_0^{\pi/2} \alpha_r(\lambda, \theta) \{1 - [\tau_s(\lambda, 0)]^{1/\cos(\theta)}\} I_b(\lambda, T_a) \sin(2\theta) d\theta d\lambda \\
q_{sun} = G \dfrac{\int_0^{+\infty} \alpha_r(\lambda, \theta_{sun}) I_{AM1.5}(\lambda) d\lambda}{\int_0^{+\infty} I_{AM1.5}(\lambda) d\lambda}
\end{cases}
$$

$$(14)$$

Here, four different radiators, including ideal radiators, were selected for cooling potential prediction. The radiative properties of the radiators are presented in Fig. 4. Radiator A is a narrowband-ideal radiator with high emissivity only within the sky atmospheric window, whereas radiator B is a broadband-ideal radiator with high emissivity in the entire mid-infrared band (i.e., over 4 μm). The two other radiators were also created by adding 5% solar absorption to radiators A and B. During the prediction process, ambient temperature and solar radiation were set as 300 K and 800 W·m⁻², respectively. The transmittance profile of the sky atmosphere was provided by Ref. [53] and the intrinsic cooling loss was assumed to be eliminated.

The cooling potentials of different radiators and several pieces of vital information are presented in Fig. 5. First, the minimum temperature of the narrowband-ideal radiator, which is achieved by passive radiative cooling, is largely lower than that of the broadband-ideal radiator. For example, the minimum temperature of radiator A is approximately 206 K whereas that of radiator B is approximately 253 K. Second, the maximum cooling power of the broadband-ideal radiator, which is obtained when $T_r = T_a$, is approximately 160 W·m⁻² and is higher than that of the narrowband radiator. Based on the preceding results, the narrowband-ideal radiator is the best choice for obtaining sub-ambient cooling phenomenon, whereas the broadband-ideal radiator can dissipate considerable waste energy into the universe when the operating temperature of the radiator is near or higher than the ambient temperature. Third, the cooling performance of the radiator is decreased and/or even damaged by parasitic solar absorption of the radiator, which can be easily realized from the comparison of related curves in Fig. 5.

3. Material and structure of radiators

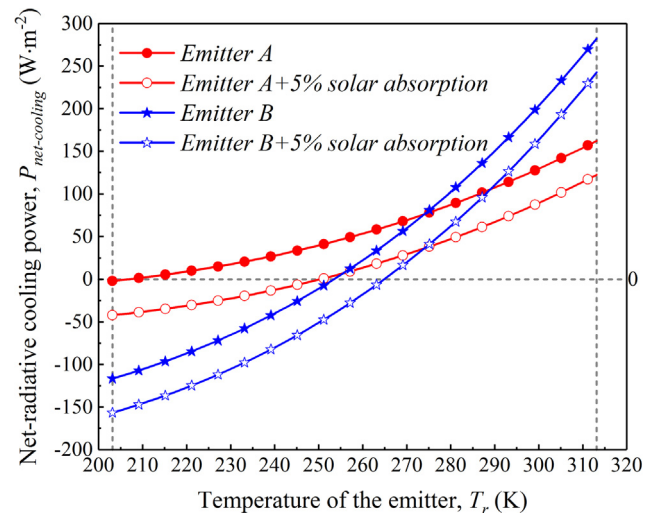Based on the basic cooling principles of radiative cooling, the

Fig. 5. Cooling potentials of different radiators. During the prediction process, ambient temperature and solar radiation were set as 300 K and 800 W·m⁻², respectively. The transmittance profile of the sky atmosphere was provided by Ref. [53] and the intrinsic cooling loss was assumed to be eliminated.

radiative property of the radiator is proven to be one of the key parameters for efficient radiative cooling. Historically, naturally available materials and synthetic polymers were pioneers for radiative cooling. Moreover, various energy-efficient radiators, including pigmented paints [54] and functional film-coated radiators (e.g., silicon monoxide SiO and silicon nitride Si₃N₄) [55–57], were continuously developed for nocturnal radiative cooling. However, these radiators with strong emission in the atmospheric window and/or entire thermal radiation band do not have high reflectivity for solar radiation, thus limiting the applications of most radiators during daytime. With recent progress in micro/nanomaterials, new materials and structures, such as photonic structures [13], nanoparticle-doped materials [58], and metamaterials [59], were designed and fabricated for diurnal radiative cooling. Thus, commonly used and advanced radiators for nocturnal and diurnal radiative cooling are summarized, classified, and discussed in this section.

3.1. Natural radiators

Radiative cooling can generally be illustrated by natural phenomenon, such as frost and dew water formation on leaves (Fig. 6(a)) [60–62]. The frost and dew water are observed to be formed on the sky-faced surface of the leaf even when the freezing and dew-point
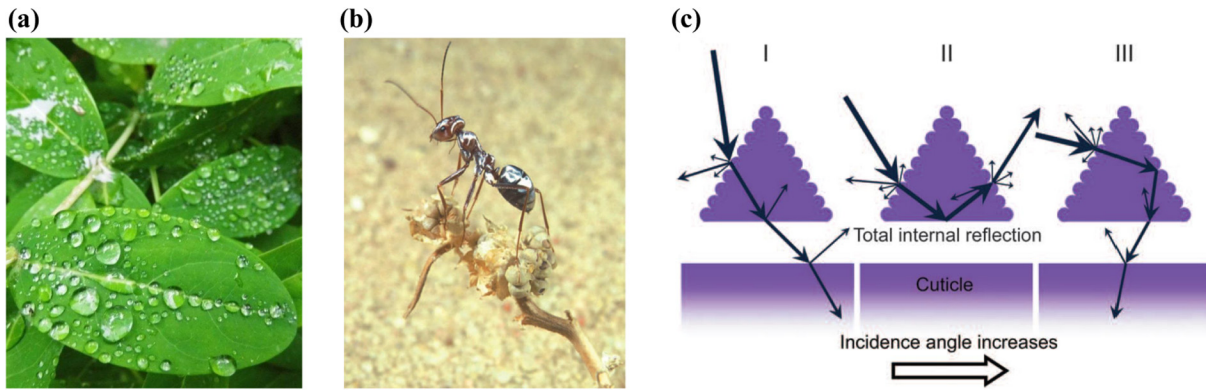
Fig. 6. Nature radiators for radiative cooling. (a) Dew water formation on leaves. (b)–(c) Photo of a silver ant and schematic diagram of its structure basis [63].

temperatures are not reached. Moreover, some animals can passively cool themselves by the outer surface of their bodies. For example, the silvery appearances of Saharan ants (Fig. 6(b) and (c)) were revealed to have excellent solar reflection and strong IR thermal emission that maintains their cool temperature even at a hot desert [63]. After analyzing the relation between radiative properties of the nature radiators and their special structures, some advanced materials for radiative cooling, such as biomimetic materials, can be originally produced, which would be a good way to explore the undiscovered radiators for efficient radiative cooling.

3.2. Film-based radiators

3.2.1. Polymer film

Highly versatile polymer film-based radiators were widely selected as outstanding candidates for nocturnal radiative cooling. At the early stage, three typical polymer materials, including polyvinyl fluoride (PVF or Tedlar) [64,65], polyvinyl chloride (PVC) [66], and polymethylpentene (TPX) [67], were analyzed and applied as radiators due to their low reflectivity and transmittance in the atmospheric window, corresponding to high emissivity. The comparison of radiative properties among the three aforementioned polymers was investigated by Granqvist et al. [19] and represented in Fig. 7.

In the original research conducted by Trombe [66], PVC film was first proposed to be placed on an aluminum sheet for radiative cooling, which was proven useful for achieving sub-ambient cooling phenomenon at nighttime. In the 1970s, Catalanotti et al. [6,64] developed a novel polymer film-based radiator by coating an evaporated aluminum

plate with a thin PVF film, which has an average emissivity of 0.8–0.9 in the wavelength range of 8–13 μm and an average reflectivity of approximately 0.85 outside the region of 8–13 μm. By controlling the negative effect of cooling loss on the radiator by insulation frame and infrared-transparent cover, this radiator not only obtains cooling phenomenon at nighttime but also achieves sun-ambient cooling under diffused sunlight. Furthermore, this type of PVF-based radiator was continuously applied and developed by Landro et al. [68], Addeo et al. [69], and Berdahl et al [25], for nocturnal radiative cooling.

In recent studies, several new polymer materials, such as polydimethylsiloxane (PDMS) [52,70] and polyethylene terephthalate (PET) [71], were explored for radiative cooling. Czapla et al. [70] demonstrated that a thin film of PDMS on aluminum substrate acts as a radiator by selectively emitting in the wavelength range of 8–13 μm. The simulation results showed that the cooler can achieve passive cooling up to 12 °C below the ambient temperature under the clear night sky. Kou et al. [52] also proposed a PDMS-coated fused silica mirror for efficient diurnal radiative cooling. The outdoor experiment demonstrated that such a radiator can passively conduct radiative cooling below ambient temperature by 8.2 °C at daytime and 8.4 °C at nighttime. Furthermore, a novel spectral surface known as TPET was investigated by adding PET film on top of a conventional selective absorber (titanium-based), which exhibits high absorptivity/emissivity in solar spectrum and atmospheric window [71], respectively, as shown in Fig. 8.

All these types of polymer-based radiators exhibit two typical characteristics for efficient radiative cooling applications: first, these radiators have strong IR emission, a key factor for radiative cooling; second, the large-scale production ability of radiators, which is an excellent feature for real applications, can be potentially achieved. However, there are still several concerns for polymer based radiators in real applications. Generally, the life of these radiators should be considered and estimated because polymer materials are easy to be aged; thus, a life cycle analysis will be a useful reference. Besides, the
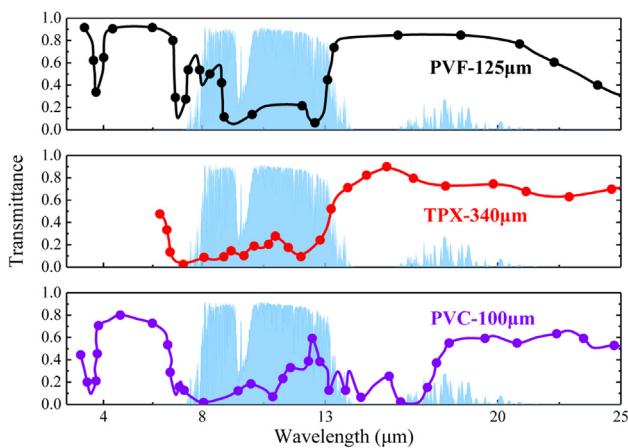

Fig.7. Spectral transmittance of three different polymer films of interest for radiative cooling with a typical atmospheric window plotted as reference. The thickness of PVF, TPX, and PVC are 125, 340, and 100 μm, respectively. The data were obtained from Ref. [19].
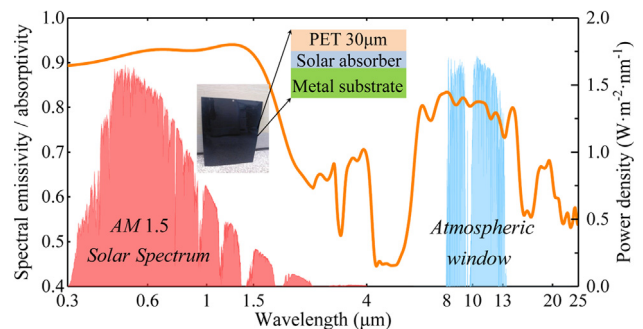

Fig. 8. Structure and spectral emissivity/absorptivity of TPET surface. The data were obtained from Ref. [71].

mechanical strength of these radiators is usually small; thus, the durability of the radiator may be a problem for actual application.

3.2.2. Pigmented paint film

In addition to polymer film, pigmented paints are a good choice of materials for spectral selective radiators. Materials, such as titanium dioxide (TiO_2) and barium sulfate ($BaSO_4$), were typically used as key constituents of pigmented paints. For example, a commercially available white paint containing 35% of titanium dioxide (TiO_2) was manufactured by Perma Paint in Calgary, Alberta [72].

Harrison and Walton [72] proposed a spectral selective radiator by coating aluminum plates with an optically thick layer of above white paint, which exactly exhibits high emissivity within the atmospheric window. Under clear sky and low absolute humidity, nocturnal radiative cooling to nearly 15 °C below the ambient air temperature was experimentally demonstrated. Michell and Biggs [73] applied TiO_2-pigmented paint on a galvanized steel surface to fabricate a "blackbody" radiator for wavelength larger than 3 μm. The cooling performance was estimated in an identical house roofed by this radiator, and net cooling power of 22 W·m^{-2} was obtained at a roof temperature of 5 °C with ambient temperature of 10 °C. An auxiliary material, $BaSO_4$, was added to the paint coating by Orel et al. [54] to improve the cooling performance of the TiO_2-based radiator. The experimental testing demonstrated that the temperature reduction was increased by 3.2 °C by $BaSO_4$-containing radiator. In the further exploration, this concept of pigmented paint-based radiator has been continuously extended and developed. By contrast, some interesting investigations were focused on the pigmented paint-based infrared cover, such as zinc sulfide (ZnS)-pigmented polyethylene [48] and zinc selenide (ZnSe)-pigmented polyethylene [49]. Although this topic is important for the development of radiative cooling, it is not further expanded in this discussion.

Considering the properties of the pigmented paints, researchers found that the pigmented paints possess the unique advantage of coating flexibility with regular paints, which is a necessary condition for realizing market applications. The aforementioned pigment paint films were usually used at nighttime for sub-ambient cooling due to their high emissivity in the atmospheric window. If the solar reflection of paint based radiator can be improved dramatically, sub-ambient radiative cooling at daytime can be achieved by this type of radiator, which will greatly increase the possibility of realizing market applications, especially for energy-saving buildings.

3.2.3. Inorganic coating film

Another choice of film-based radiators for radiative cooling is inorganic coating, especially silicon-related ones such as silicon monoxide (SiO), silicon dioxide (SiO_2), silicon carbide (SiC), silicon nitride (Si_3N_4), and silicon oxynitride (SiO_xN_y).

In the 1980s, Granqvist et al. [19,55,56,74] developed a series of SiO-coated radiators that perform selective emission. Materials with intrinsic high reflectivity, such as polished aluminum and silver film, were the best choice for substrate and reflective layers. For example, the radiative property (Fig. 9(a)) of SiO-coated radiators with different thicknesses was analyzed and compared by Granqvist et al. [19]. A certain thickness of approximately 1 μm corresponding to the best cooling performance was determined and a passive cooling phenomenon of 14 °C below ambient surrounding was experimentally achieved. Similarly, Si_3N_4 film [57], $SiO_{0.6}N_{0.2}$ film [75,76], and double films of SiO_2- and $SiO_{0.25}N_{1.52}$-based [77] radiators were also designed, fabricated, and studied by Granqvist et al. The spectral characteristics of these radiators are presented in Fig. 9.

Notably, SiO_2 is a special and preeminent material of interest for radiative cooling, which has been widely investigated and applied. The optical property, which consists of refractive index and extinction coefficient, is given in Fig. 10(a), where two vital messages are observed. First, the extinction coefficient of SiO_2 is zero over the entire
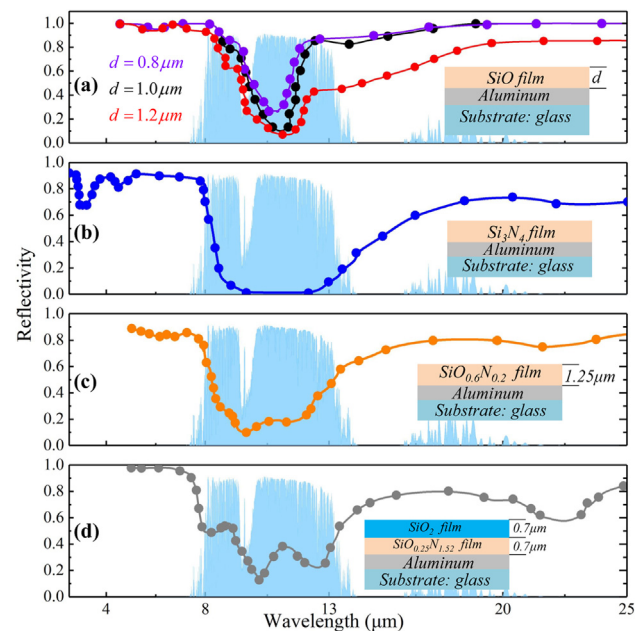

Fig. 9. Spectral reflectivity of different silicon-based coatings for radiative cooling with a typical atmospheric window plotted as reference. Notably, the spectral reflectivity profile presented in (d) is computed under a fixed incident angle of 45°. All the data were obtained from the following: (a) Ref. [19], (b) Ref. [57], (c) Ref. [75], and (d) Ref. [77].

solar radiation band, indicating that SiO_2 is physically transparent for solar radiation, which is one of the perfect features for achieving sub-ambient radiative cooling at daytime. Second, SiO_2 has two strong peaks in its extinction coefficient near 10 μm and 20 μm, where the special effect of the phonon-polariton resonances exists. For bulk materials, including coatings, a strong impedance mismatch between the interface of SiO_2 and air is produced at these bands, thereby resulting in large reflectivity (Fig. 10(b)) of the interface and a negative effect for thermal emission enhancement. However, thin SiO_2 coatings are semi-transparent for IR emission. Thus, two typical applications of SiO_2, including thin film and thick bulk materials, were developed for radiative cooling. The spectral emissivity of two similar configurations with a 1.8 μm-thick SiO_2 film and a 500 μm-thick bulk SiO_2 were calculated and presented in Fig. 10(c).

Apart from silicon-based coatings, numerous special interest inorganic coatings are available for radiative cooling. Berdahl [79] estimated the potential of magnesium oxide (MgO) and/or lithium fluoride (LiF) as radiator for sub-ambient radiative cooling and experimentally obtained a net cooling power of more than 85 W·m^{-2} on a clear night sky.

3.3. Nanoparticle-based radiators

Compared with bulk materials, nanoparticles have optical properties that may be slightly different. For example, the phonon-polariton resonances of bulk SiO_2 can result in a strong reflection peak; by contrast, this effect can be induced to be a remarkable absorption by SiO_2 particles, corresponding to strong emission. Thus, the nanoparticle-based radiator is one of the candidates for efficient radiative cooling.

Bao et al. [21] proposed a highly scalable nanoparticle-based double-layer coating radiator (Fig. 11(a)), which exhibits selective properties for radiative cooling. This radiator mainly consists of a top reflective layer and a bottom emissive layer comprising titanium dioxide (TiO_2) nanoparticles and SiO_2 and/or SiC nanoparticles, respectively, which are responsible for reflecting solar radiation and emitting heat into outer space. For cooling performance, 17 °C and 5 °C below ambient air temperature at nighttime and daytime were theoretically
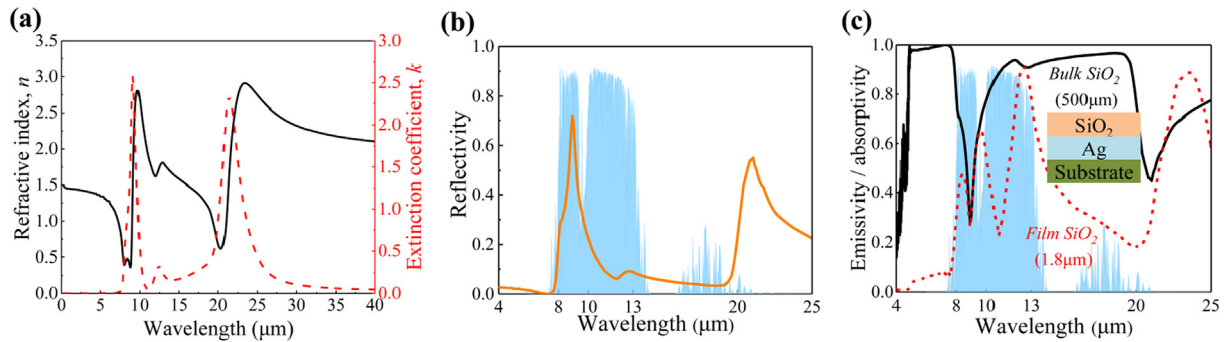
Fig. 10. Optical properties of SiO₂ material. (a) Refractive index and extinction coefficient of SiO₂ (glass). The data were obtained from the handbook of optical constants of solids [78]. (b) Spectral reflectivity of the SiO₂ film, which is independent of the thickness. (c) Spectral emissivity/absorptivity of a specific configuration with a SiO₂ film on top. A bulk SiO₂ (500 μm) and a film SiO₂ (1.8 μm) were selected as the corresponding top layer.
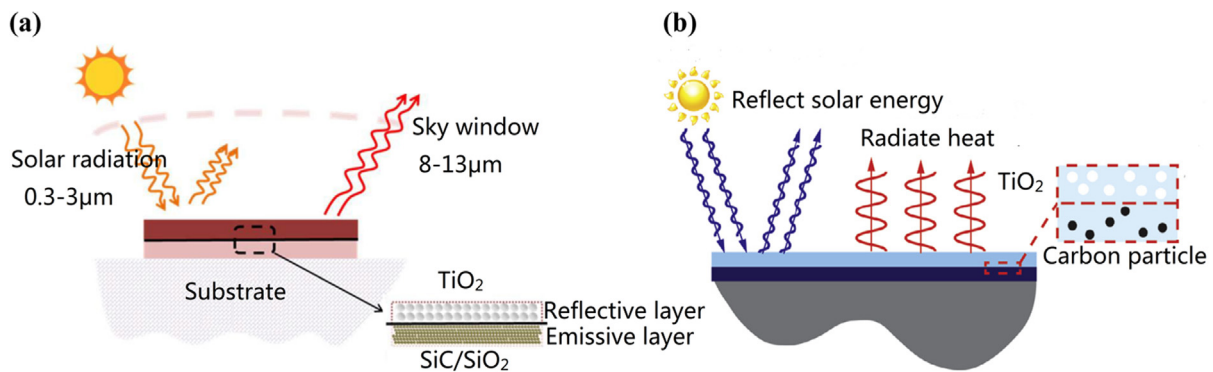
Fig. 11. Two typical nanoparticle-based double-layer coatings. (a) From Ref. [21]. (b) From Ref. [58].
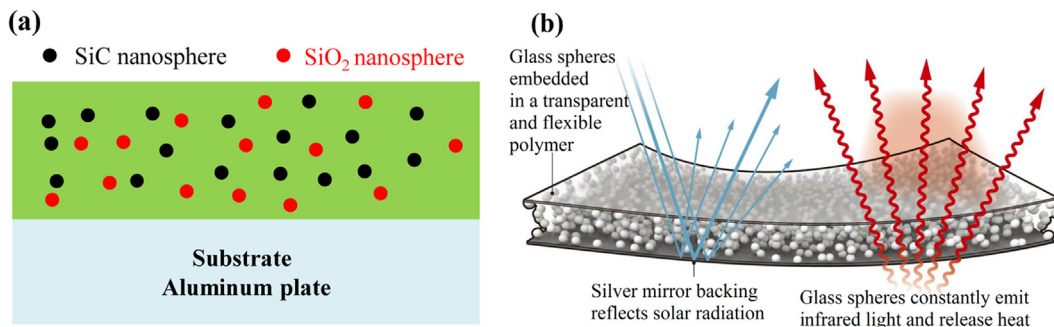
Fig. 12. Two typical nanoparticle-doped polymer radiators. (a) From Ref. [80], (b) From Ref. [81].
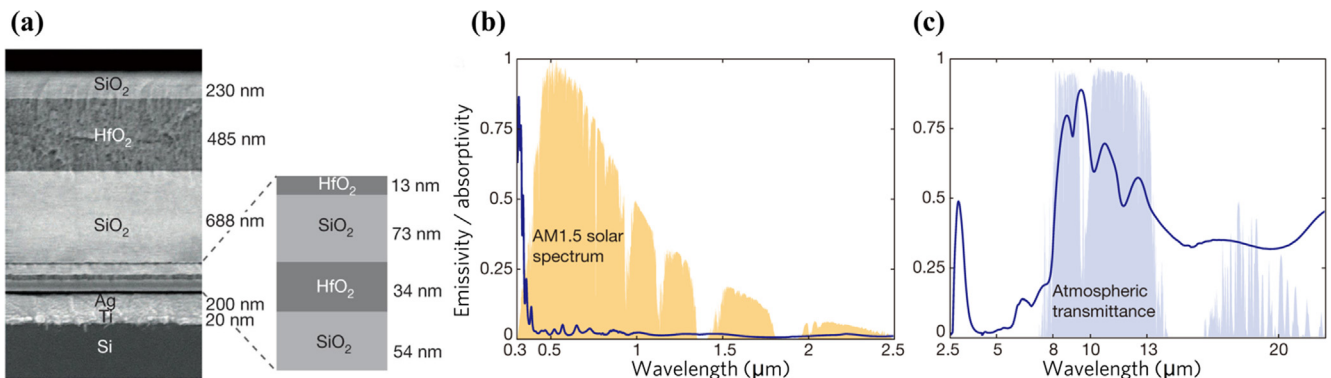
Fig. 13. Scanning electron microscope and spectral characterizations of a photonic radiator (multilayer film) reported in Ref. [13].
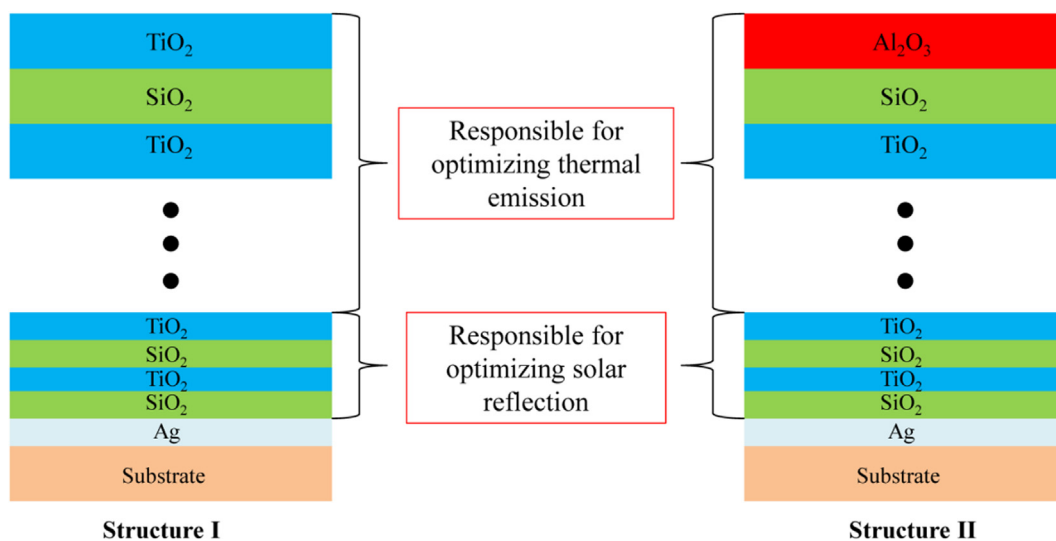
Fig. 14. Schematic of new design multilayer structures reported in Ref. [83].
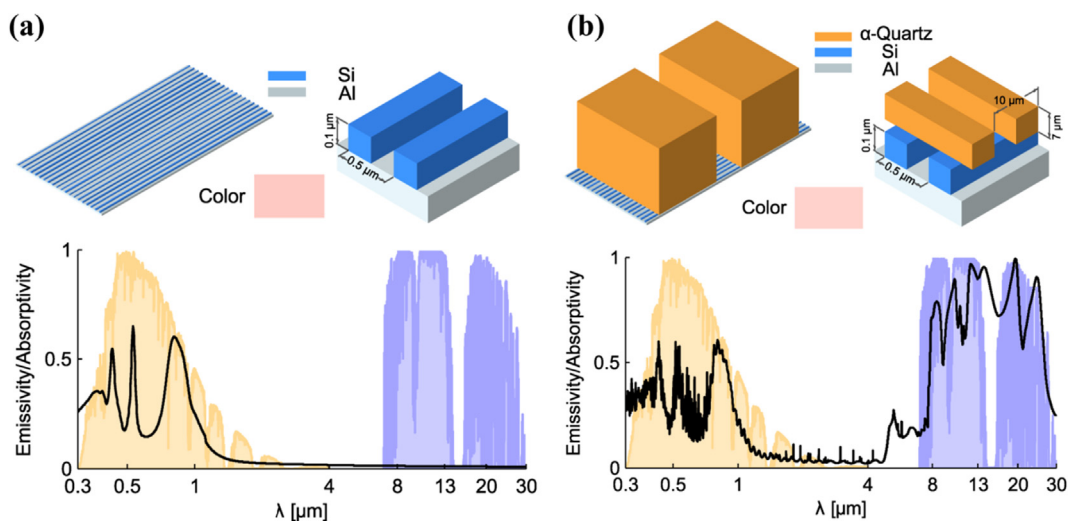
Fig. 15. Schematic of approach reported in Ref. [93] for color-preserving diurnal radiative cooling. (a) Schematic of original structure with silicon nanostructure used as color creator. (b) Schematic of modified structure with α-quartz bar array on top of the original structure for strong thermal emission.
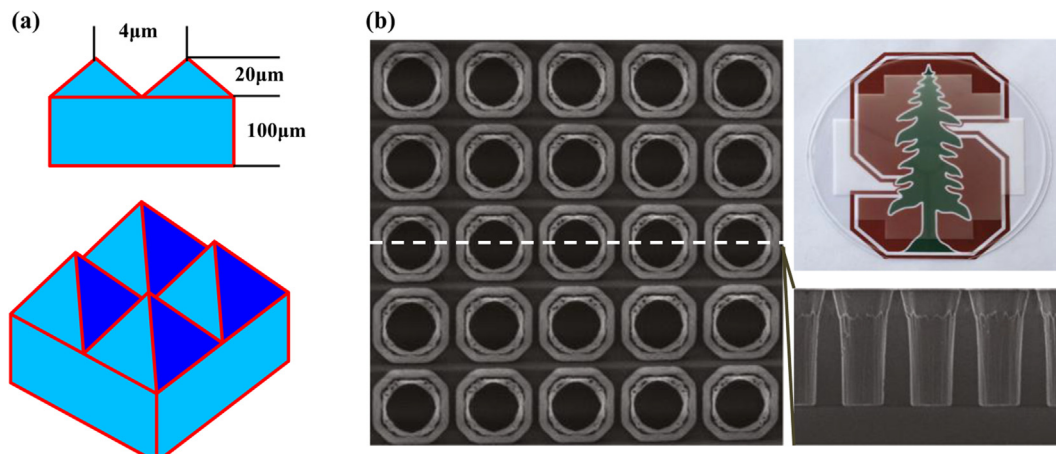
Fig. 16. Structure of photonic radiator reported in Refs. [20] and [95]. (a) Schematic of 2D square lattice of silica pyramids on a uniform silica layer. (b) SEM image and photo of photonic radiator comprising square lattice air holes on a bulk silica material.

(a)

(b)
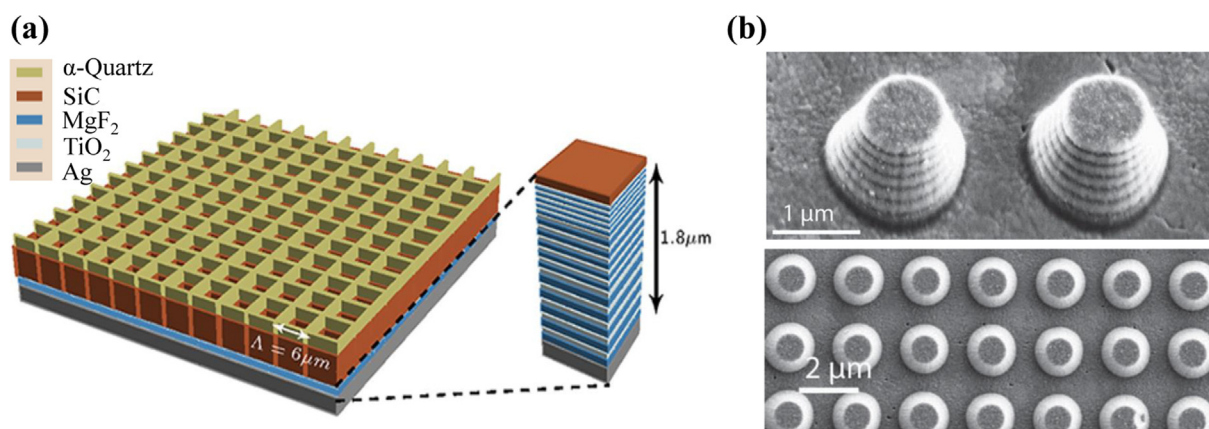
Fig. 17. Combination structures of patterned surface and multilayer reported in Refs. [97] and [98], respectively. (a) Schematic of radiator that consists of a two-layer 2D patterned surface for thermal radiation and a chirped multilayer for solar reflection. (b) SEM image of photonic radiator that consists of an array of CMM structures.

achieved under a dry sky condition, respectively. A similar radiator was developed by embedding TiO_2 and carbon black particles into acrylic resin to be a double-layer coating [58], as shown in Fig. 11(b).

Some polymers, such as TPX and low-density polyethylene (LDPE), are optically transparent for solar radiation. If nanoparticles with only narrow absorption bands within the atmospheric window are doped in these polymers, then thermal emission in 8–13 μm would be enhanced while still maintaining transparency for solar radiation. Gentle and Smith [80] developed a nanoparticle-doped PE film radiator (Fig. 12(a)) that contains a mixture of SiC and SiO_2 nanoparticles in PE film, which can ensure high-performance cooling at low cost with a reflector layer (e.g., aluminum) on the back. Zhai et al. [59] randomly embedded resonant polar dielectric SiO_2 particles in a TPX matrix and developed a novel metamaterial (Fig. 12(b)) for radiative cooling. This metamaterial is fully transparent to solar radiation while possessing strong thermal emission within the atmospheric window. A diurnal net cooling power of 93 W·m^{-2} was experimentally obtained when backed with a reflector layer (silver-Ag).

Nanoparticle-based radiator is one of the innovative materials designed for radiative cooling, especially for diurnal sub-ambient radiative cooling. Thus, strict spectral selective properties are required, including high reflectivity for solar radiation and strong thermal emission within atmospheric window. Generally, high reflectivity for solar radiation is obtained by a reflective layer, which can be deposited silver layer, TiO_2 particles and so on. The strong thermal emission can be achieved using an emissive layer, such as near-black surface and particle-doped polymer.

3.4. Photonic radiators

With the recent emergence of advanced design and fabrication technologies, the photonic approach [82] has been rapidly developed for efficient radiative cooling, especially sub-ambient diurnal radiative cooling. The photonic approach facilitates the modification of the spectral radiative properties of the radiator by proper periodic structuring, including multilayer film and pattern surface, which ingeniously provide various possibilities to improve the radiative cooling abilities.

3.4.1. Multilayer film

Multilayer film, a 1D photonic crystal, is a typical photonic radiator that consists of alternating layers of material with different dielectric constants. Sub-ambient diurnal radiative cooling was first experimentally achieved by Raman et al. [13] with a multilayer film under direct sunshine. As shown in Fig. 13, this multilayer film consists of seven alternating layers of hafnium dioxide (HfO_2) and SiO_2 with various thicknesses on top of 200 nm Ag and 750 μm silicon wafer substrates,

which reflects approximately 97% of incident solar irradiance and simultaneously emits a strong thermal radiation. Outdoor experiments demonstrated that diurnal radiative cooling to 5 °C below ambient temperature was obtained and a net cooling power of approximately 40.1 W·m^{-2} was harvested at ambient temperature even under a parasitic cooling loss process.

An evolution of the above multilayer film was developed by Kecebas et al. [83] by replacing HfO_2 with TiO_2 and aluminum dioxide (Al_2O_3). The schematic of the new photonic radiators is presented in Fig. 14. Structure I is generally a modification of the original multilayer stack reported in Ref. [13], in which layers responsible for optimizing thermal emission are increased. Moreover, additional Al_2O_3 used in structure II considerably improved the thermal emission at approximately 10 μm due to its intrinsic physical absorption.

Similar multilayer films have been widely developed for radiative cooling. For example, Gentle and Smith [84] established a multilayer polymer material that uses multiple birefringent polymer pairs to demonstrate diurnal radiative cooling under open condition. Huang et al. [85] designed an "invisible" radiative cooling coat comprising seven alternating layers of calcium fluoride (CaF_2) and germanium (Ge) on top of a thin nichrome metal film followed by a layer of dielectric spacer and a reflector.

For the multilayer film, the number and thickness of the layer are the vital parameters for spectral tailoring. From a theoretical viewpoint, various classical methods are available for the design and optimization of the multilayer film, such as needle optimization [86,87], simulated annealing [88], jump method [89], memetic algorithm [90], and et al. Moreover, some commercial tools for practical application, including TFCalc [91] and Essential Macleod [92], have been developed for film design. By contrast, many techniques have also been applied for film fabrication, such as sputtering, atom layer deposition, and et al. However, during the process of multilayer film fabrication, the thickness error of the individual layer cannot be eliminated, which will harm the optimized optical properties of the multilayer film, especially for those that are sensitive to thickness. Thus, a multilayer film with a suitable number and thickness of layers will be popular with real applications.
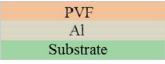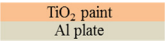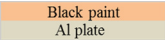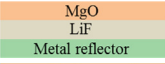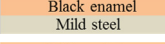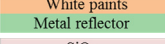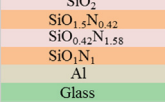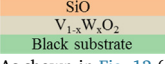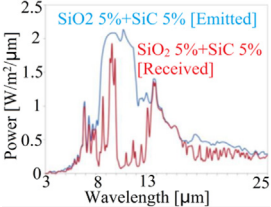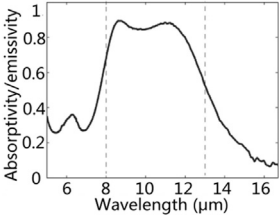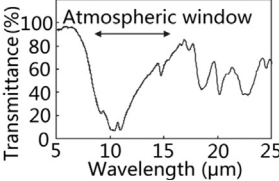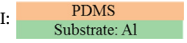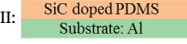
3.4.2. Patterned surface

In addition to the multilayer film, a patterned surface has been developed as photonic radiator for efficient radiative cooling. Compared with the multilayer film, the patterned surface has a high degree of freedom, which is a good feature for tailoring the spectral selectivity of the surface. Recent progress on the patterned surface for radiative cooling is reviewed in this section.

Zhu et al. [93] proposed a general strategy for achieving color-preserving diurnal radiative cooling by using an α-quartz
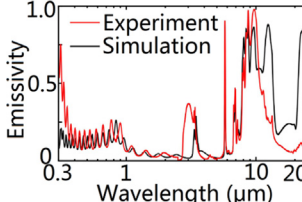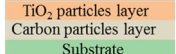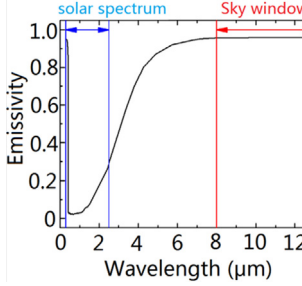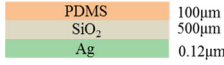
Table 3
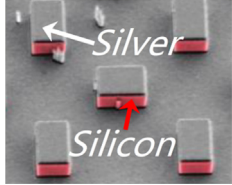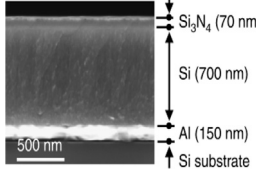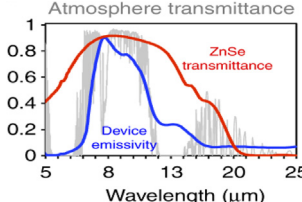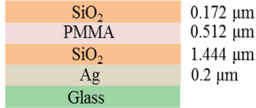
Summary of materials, structures, and radiative properties of radiator. (*Note:* The symbols √, ×, and − *in the column "Modes" represent radiators were designed for sub-ambient nighttime cooling, sub-ambient daytime cooling and purely heat dissipation, respectively.*)

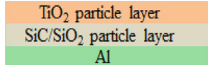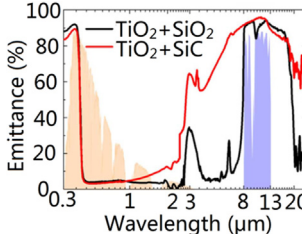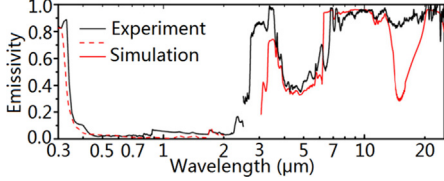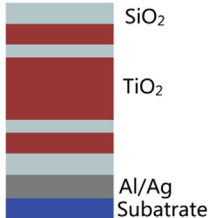| Modes	Authors	Structures/materials	Radiative property
√	Johnson [99]	Plexiglass	N/A
√	Granqvist et al. [55]	As shown in Fig. 9(a)	As shown in Fig. 9(a)
√	Natsui et al. [61]	Nature leaf	N/A
√	Hjortsberg et al. [100] Lushiku et al. [23] Lushiku et al. [101]	Ethylene gas (C_2H_4) Ethylene oxide gas (C_2H_4O) Ammonia gas (NH_3)	N/A
√	Granqvist et al. [57]	As shown in Fig. 9(b)	As shown in Fig. 9(b)
√	Eriksson et al. [75] Eriksson et al. [77]	As shown in Figs. 9(c) and (d)	As shown in Figs. 9(c) and (d)
√	Hu et al. [71]	As shown in Fig. 8	As shown in Fig. 8
√	Dan et al. [102]	Glass used in solar collector	The hemispherical emissivity is approximately 0.84
√	Etzion et al. [103]	Polycarbonate	The infrared emissivity is approximately 0.95
√	Catalanotti et al. [6] Bartoli et al. [64] Addeo et al. [65] Berdahl et al. [25]	PVF / Al / Substrate	The reflectivity in 8–13 µm is 0.1–0.2 and is approximately 0.85 outside 8–13 µm
√	Harrison et al. [72] Michell et al. [73]	TiO_2 paint / Al plate	N/A
√	Landro et al. [68] Ito et al. [104] Hamza et al. [105]	Black paint / Al plate	The hemispherical emissivity is within 0.8–0.9
√	Berdahl [79]	MgO / LiF / Metal reflector	The emissivity is about 0.9 within 8–14 µm
√	Ezekwe [106] Ezekwe [107]	Black enamel / Mild steel	The hemispherical emissivity is approximately 0.9
√	Orel et al. [54]	White paints / Metal reflector	The emissivity within 8–13 µm is about 0.9
√	Diatezua et al. [108]	SiO_2 / $SiO_{1.5}N_{0.42}$ / $SiO_{0.42}N_{1.58}$ / SiO_1N_1 / Al / Glass	The emissivity is about 0.77 within 8–13 µm
√	Tazawa et al. [109] Tazawa et al. [110]	SiO / $V_{1-x}W_xO_2$ / Black substrate	N/A
√	Gentle et al. [80]	As shown in Fig. 12 (a)	
√	Hossain et al. [98]	As shown in Fig. 17 (b)	
√	Miyazaki et al. [111]	Si_2N_2O coating	
√	Czapla et al. [70]	I: PDMS / Substrate: Al II: SiC doped PDMS / Substrate: Al	The emissivity is 0.7–0.9 within 8–13 µm
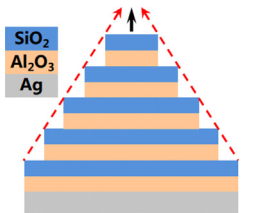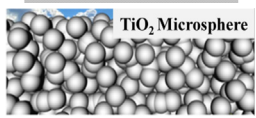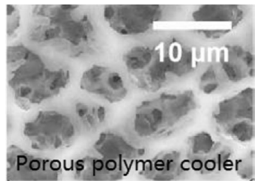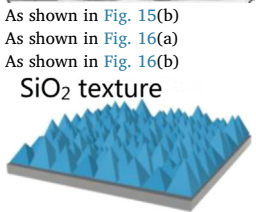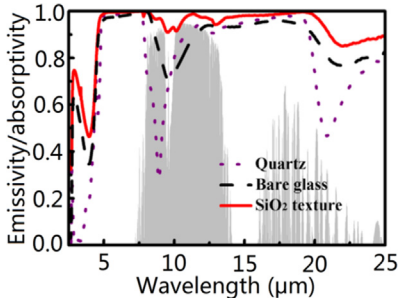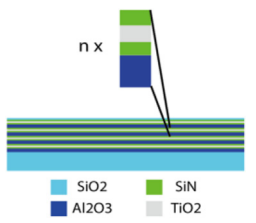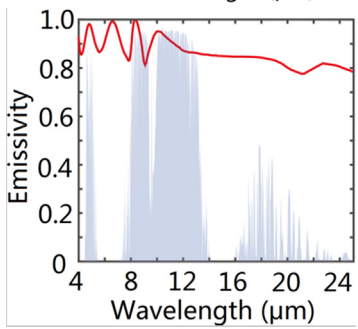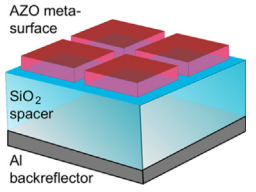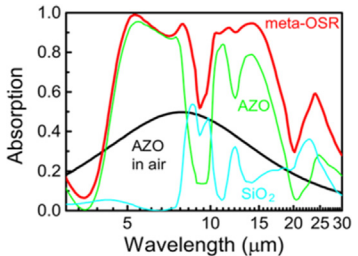
(*continued on next page*)

Table 3 (*continued*)

Modes	Authors	Structures/materials	Radiative property
√	Zou et al. [112]		The emissivity is about 0.85 within 8–13 μm
×	Raman et al. [13]	As shown in Fig. 13(a)	As shown in Fig. 13(b) and (c)
×	Gentle et al. [84]	Multiple birefringent polymer pairs	Solar reflection is 0.97 and emissivity within 8–13 μm is approximately 0.96
×	Kecebas et al. [83]	As shown in Fig. 14	N/A
×	Rephaeli et al. [97]	As shown in Fig. 17(a)	Solar reflection is about 0.96 and emissivity is selectively high within atmospheric window
×	Chen et al. [45]		
×	Suichi et al. [113]		
×	Huang et al. [58]		
×	Kou et al. [52]		Near-blackbody in mid-infrared band
×	Bao et al. [21]		
×	Zhai et al. [59]	As shown in Fig. 12(b)	
×	Wu et al. [114]		Strongly reflect sunlight and selectively emissive within 8–13 μm

Table 3 (continued)

Modes	Authors	Structures/materials	Radiative property
×	Wu et al. [96]	SiO2 / Al2O3 / Ag	Near-blackbody within 8–30 μm
×	Atiganyanun et al. [115]	TiO2 Microsphere	Strong solar reflection with an average emissivity larger than 0.94 in atmospheric window
×	Mandal et al. [116]	10 μm Porous polymer cooler	Solar reflection is 0.96 ± 0.03 and thermal emissivity is 0.97 ± 0.02
−	Zhu et al. [93]	As shown in Fig. 15(b)	As shown in Fig. 15(b)
−	Zhu et al. [20]	As shown in Fig. 16(a)	Near-blackbody in mid-infrared band
−	Zhu et al. [95]	As shown in Fig. 16(b)	Near-blackbody in mid-infrared band
−	Lu et al. [117]	SiO2 texture	
−	Li et al. [22]		
−	Sun et al. [118]	AZO meta-surface / SiO2 spacer / Al backreflector	

nanostructure, as shown in Fig. 15. An array of α-quartz bars was placed on the top of the original structure, which is transparent for solar radiation, while remaining strongly emissive in the atmospheric window, resulting in a temperature reduction. Substantial cooling while preserving the original color can be simultaneously realized with this approach, which can be a meaningful tool for various potential applications, such as outdoor or technical clothing. The similar thermal management of colored objects was achieved by Li et al. via a

multilayer photonic radiator [94].

Moreover, two other patterned surfaces that exhibit strong thermal emission in almost the entire mid-infrared wavelength band while maintaining its solar transparency were proposed by Zhu et al. [20,95]. The detailed structures are represented in Fig. 16. The basic prototype of the preceding surfaces is a bulk material of SiO$_2$, which has two main phonon-polariton resonances near 10 and 20 μm, corresponding to large reflectivity and small emissivity of the surface. However, the small
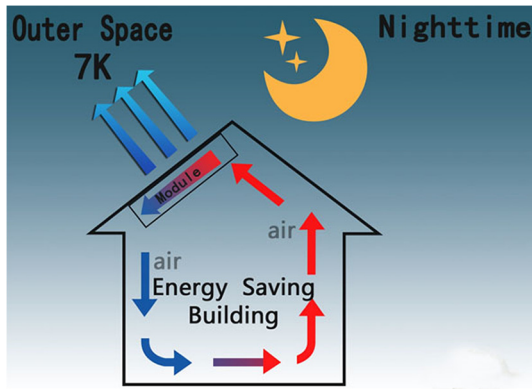
Fig. 18. Schematic of air-based radiative cooling system.

emissivity near 10 μm coincides with the peak thermal radiation of a blackbody at typical ambient air temperature, which certainly has a negative effect on radiative cooling. Two nano/microstructures, including air holes [95] and pyramids [20], were developed for bulk SiO_2 to modify this defect. Similar to pyramid patterned surface, a novel photonic radiator was proposed by Wu et al. [96] based on the moth-eye effect of micro-pyramid structure arrays comprising aluminum oxide/silica all-dielectric multilayers, which can realize extremely low solar absorption and strong thermal emission within 8–26 μm.

The combination of patterned surface and multilayer is also a useful approach for the radiator design. Rephaeli et al. [97] first reported a design of spectral selective radiator with high emissivity in the atmospheric window using a combination of a two-layer 2D patterned surface and a chirped multilayer (Fig. 17(a)). This concept was also applied by Hossain et al. [98] by utilizing a special patterned surface that consists of an array of symmetrically shaped conical metamaterial (CMM) pillars (Fig. 17(b)), each comprising multilayers of Al and Ge, resulting in a near ideal emission in the 8–13 μm wavelength range.

The photonic radiator is a hot research topic for radiative cooling due to its unique ability to tailor the spectral properties of the radiator for efficient daytime radiative cooling, which promote the development of sub-ambient radiative cooling in recent years. However, some challenges for the photonic radiator still exist. The manufacturing procedure of photonic radiator, especially for 3D radiator, is awfully demanding; thus, the cost issue of the photonic radiator is a big challenge for actual application. Besides, the large scale production is difficult to achieve at present, which is limited by crafts and facilities. Therefore, photonic radiator is still in the early development stage, which is restricted to laboratory research and exploration.

Fig. 20. Schematic of flat-plate radiative cooling system reported in Ref. [122].

3.5. Brief summary

In this section, the information on different radiators for efficient radiative cooling in previous studies was compiled and summarized in Table 3 for reference and comparison in a specific order of radiators' design purposes and working modes.

4. Application developments and prospects

Radiative cooling promises a vital impact with its excellent passive cooling potential, which can be applied in various fields, including energy-efficient buildings, photovoltaic cooling, and energy harvesting. In this section, the application developments and prospects of radiative cooling are summarized and compiled.

4.1. Energy-efficient buildings

Building energy consumption accounts for approximately 40% of the total energy consumption of the world, where a large amount of

Fig. 19. Schematic and actual photo of roof pond reported in Ref. [121].
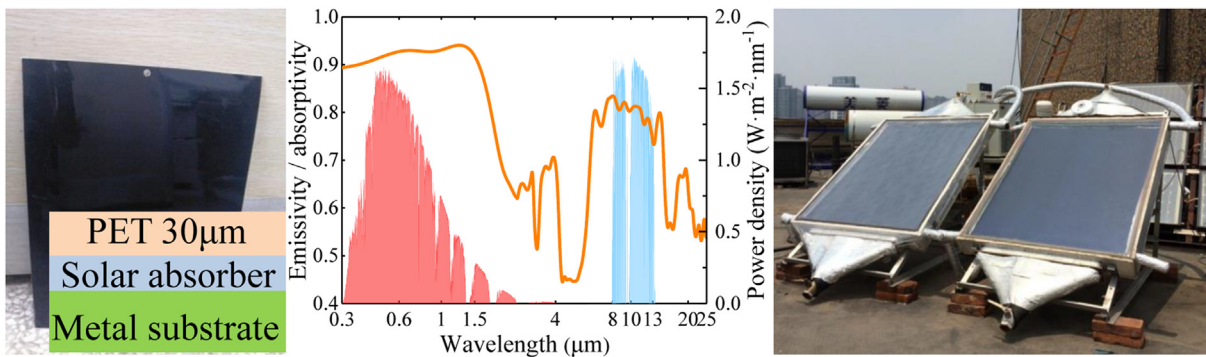
Fig. 21. Actual photo of spectral selective composite surface and PT-RC hybrid system reported in Ref. [71].
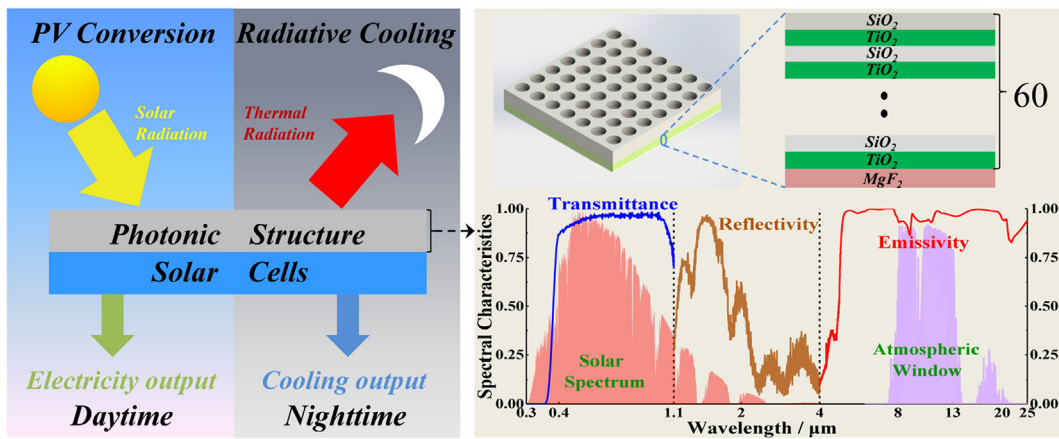
Fig. 22. Schematic and a novel panel of PV-RC utilization [127]
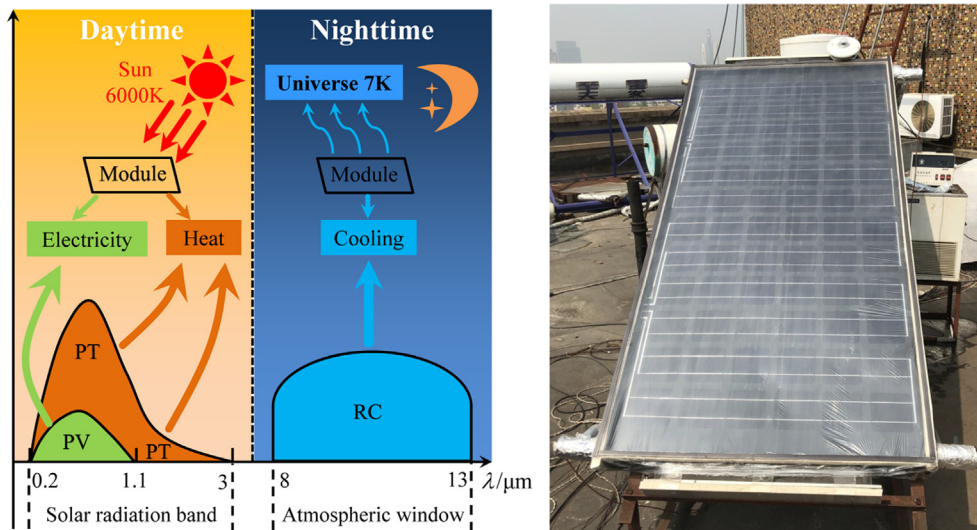
Fig. 23. Schematic and photo of PV-PT-RC utilization [132].

energy is used for indoor thermal management via conventional HVAC systems [119]. Therefore, passive radiative cooling method that cools objects without additional energy input can make a difference in establishing energy-efficient buildings. The topic of passive radiative cooling for energy-saving buildings has been reviewed by Nwaigwe et al. [120] and Lu et al. [15]. Thus, in this part, a concise description of simple concepts and typical cooling system for building integrated radiative cooling system is presented.

Nocturnal radiative cooling system has been widely applied and investigated in practice. According to the operation model of the

cooling process, the building integrated radiative cooling system can be divided into three typical categories, which are demonstrated in the following:

(1) Air-based cooling system

As shown in Fig. 18, in the air-based cooling system, air is used as the heat exchange media that is directly heated by the indoor environment and cooled by the radiator. The cooling effect of this system is notably limited for real application. If air is circulated by natural
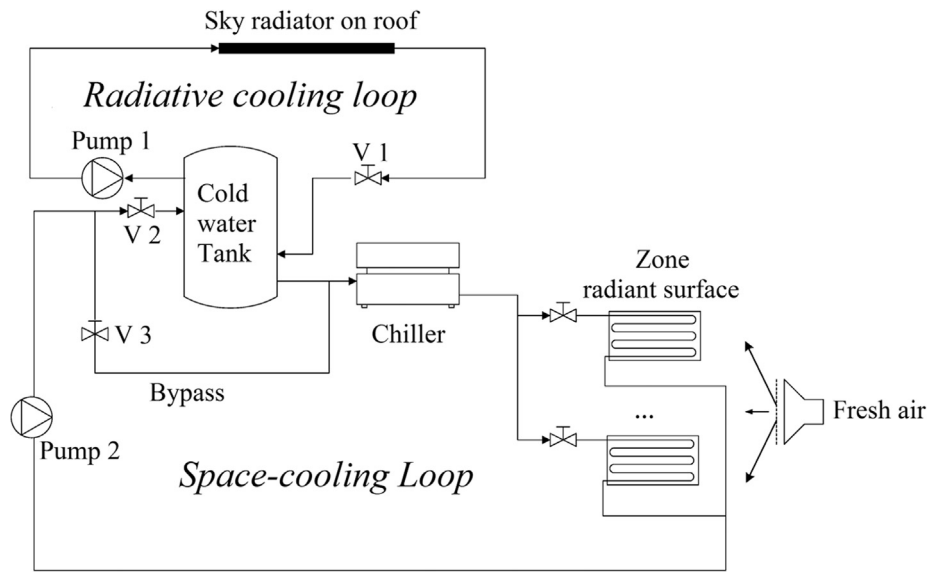
Fig. 24. Schematic of diurnal radiative cooling system [134].
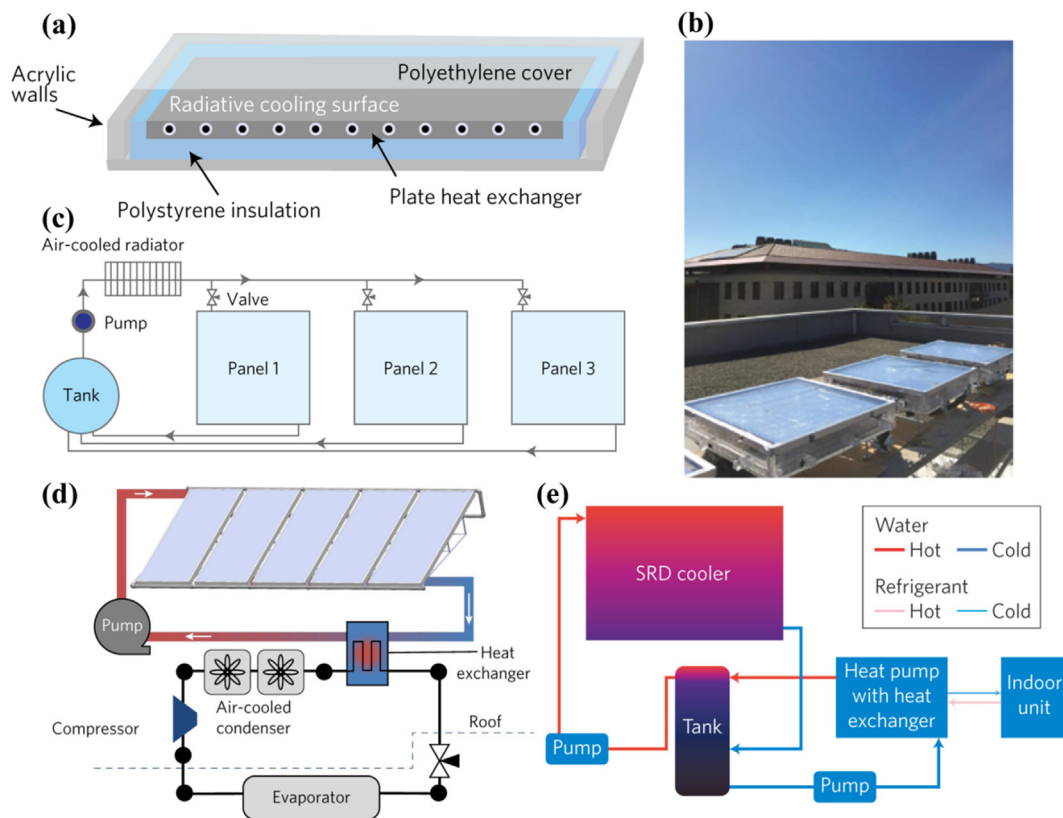
Fig. 25. Schematic of diurnal radiative cooling integrated for buildings. (a)–(d) Schematic and photo of sub-ambient non-evaporative cooling system and its integration for conventional cooling system for buildings, as reported in Ref. [135]. (e) Schematic illustration of a novel integration of diurnal radiative cooling into an conditioning system taken from Ref. [136].

buoyancy, then the effect of heat exchange between air and radiator is limited, corresponding to a small reduction in air temperature. By contrast, if air is forced by a mechanical fan to increase the net cooling power of the system, then the additional electricity is consumed by fan operation. However, the structure, operation mode, and initial cost of the air-based cooling system are friendly, which is a vital advantage for real applications.

(2) Water-based cooling system

Similarly, in the water-based cooling system, the water acts as the heat transfer media, which definitely increases the net radiative cooling power of the system. Moreover, the water-based cooling system can be easily controlled and operated due to the higher heat capacity of water compared with that of the air-based cooling system. In previous studies, two operating modes, namely, open and closed system, were developed for the water-based cooling system. For example, roof pond (Fig. 19) [121] is one of the typical open systems; meanwhile, flat-plate radiative system (Fig. 20) [122] is a representative of closed systems.
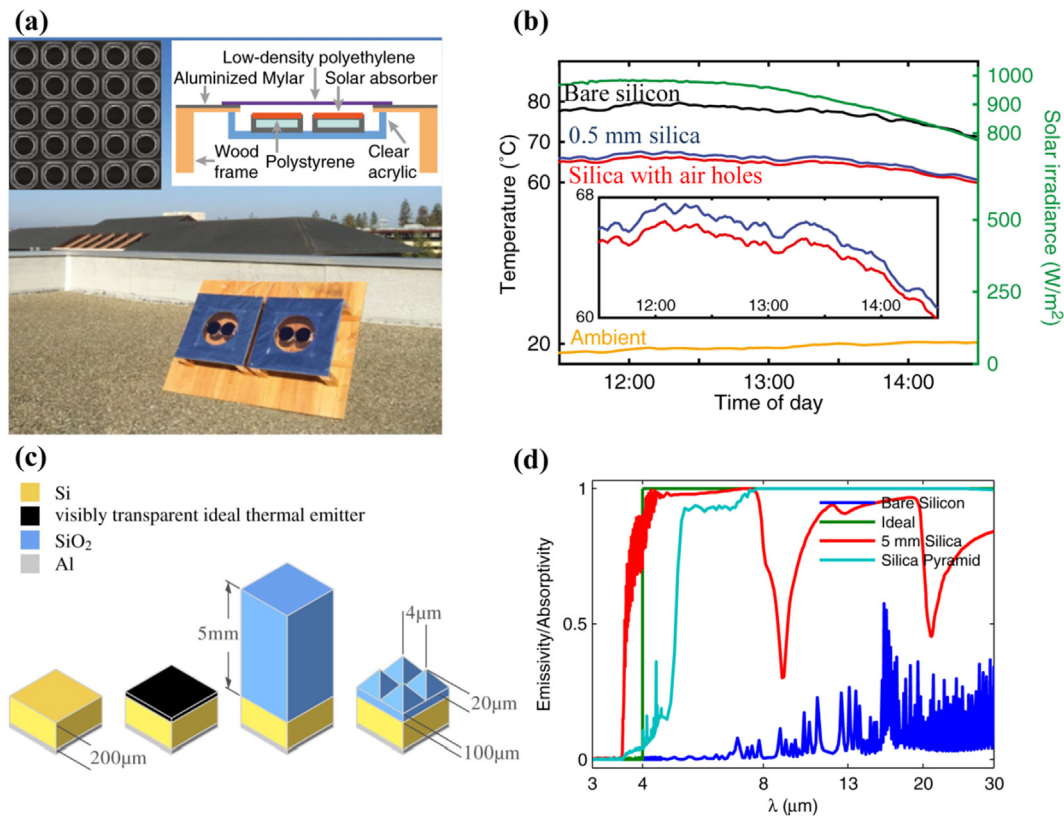
Fig. 26. Schematic of photovoltaic cooling. (a)–(b) Schematic and photo of photonic silica radiator for PV cooling, as reported in Ref. [95]. (c)–(d) Schematic and spectral characterization of a pyramid silica radiator for photovoltaic cooling with corresponding illustration of planner silica radiator and ideal radiator taken from Ref. [20].

(3) Hybrid system

The aforementioned air- and water-based cooling systems are both single units only for radiative cooling. Hybrid system, which is essentially a comprehensive combination of nocturnal radiative cooling and other energy-harvesting processes, is more energy-efficient than these systems. The previous literature shows that various hybrid systems, such as radiative and evaporative cooling (RC-EC) [123–125], radiative cooling and heat pump (RC-HP) [126], and radiative cooling and solar energy utilization (RC-SE) [44,46,71,127–131], have been investigated and developed. Specifically, RC-SE hybrid system has attracted considerable attention in recent years, especially the spectral selective-based RC-SE system. Hu et al. [71] proposed a composite surface and related system (Fig. 21) for diurnal photothermal conversion and nocturnal radiative cooling (PT-RC). The outdoor tests showed that the thermal efficiency and net cooling power of the system can reach 62.7% and 50.3 W·m^{-2}, respectively.

Apart from photothermal conversion, photovoltaic conversion can also be integrated with nocturnal radiative cooling. Zhao et al. [44,127] proposed a concept of diurnal photovoltaic and nocturnal radiative cooling hybrid system (PV-RC) and designed a novel panel for PV-RC utilization (Fig. 22). This is an interesting concept of the hybrid system for harvesting both electricity and cooling energy, which is suitable for buildings in hot regions.

If photovoltaic conversion, photothermal conversion, and radiative cooling are integrated, and then a new hybrid system called PV–PT–RC [46,132] is obtained. As shown in Fig. 23, for the silicon-based PV–PT–RC system, photons with energy higher than 1.1 eV (for silicon solar cell) will be partly converted to electricity, while the remaining absorbed photons will be transformed into heat. Moreover, cooling energy and/or space cooling can be obtained via nocturnal radiative cooling.

The above three RC-SE hybrid utilizations, including PT-RC, PV-RC, and PV-PT-RC, are novel concepts of combination of radiative cooling and solar energy. The basic response wavelength band of PV, PT, and RC are quietly different; thus, if the spectral properties of the surface for different physical process are considered and satisfied simultaneously, the overall energy efficiency and time availability will be enhanced dramatically. At present, the polyethylene film is widely selected as convection cover, but its mechanical strength is not enough, which is the main problem for using these hybrid systems in real applications.

With the development of diurnal radiative cooling, some new concepts of building integrated diurnal radiative cooling [133–136] have been investigated. Wang et al. [134] proposed a photonic radiative cooling system (Fig. 24) for office buildings and estimated the corresponding energy savings. Simulation results showed that the electricity saving is between 45% and 68% relative to conventional cooling methods. Goldstein et al. [135] experimentally demonstrated a diurnal non-evaporative fluid radiative cooling system (Fig. 25(a)–(d)) that passively achieves 5 °C below ambient air temperature. Moreover, further simulation study indicated that the electricity for cooling demand during the summer will be reduced by over 20% when this system is integrated with a conventional HVAC system for an office building. A similar idea of diurnal radiative cooling and air-conditioning integration (Fig. 25(e)) was also proposed by Smith et al. [136]. For these daytime passive cooling systems, hard convection cover is a necessary point for actual applications.

4.2. Photovoltaic cooling

The photovoltaic (PV) conversion efficiency of solar cell is limited due to the physical properties of cells. For example, the maximum efficiency of a single-gap p–n junction solar cell is approximately 33.7% based on the analysis by Shockley and Queisser [137]. Therefore, only a
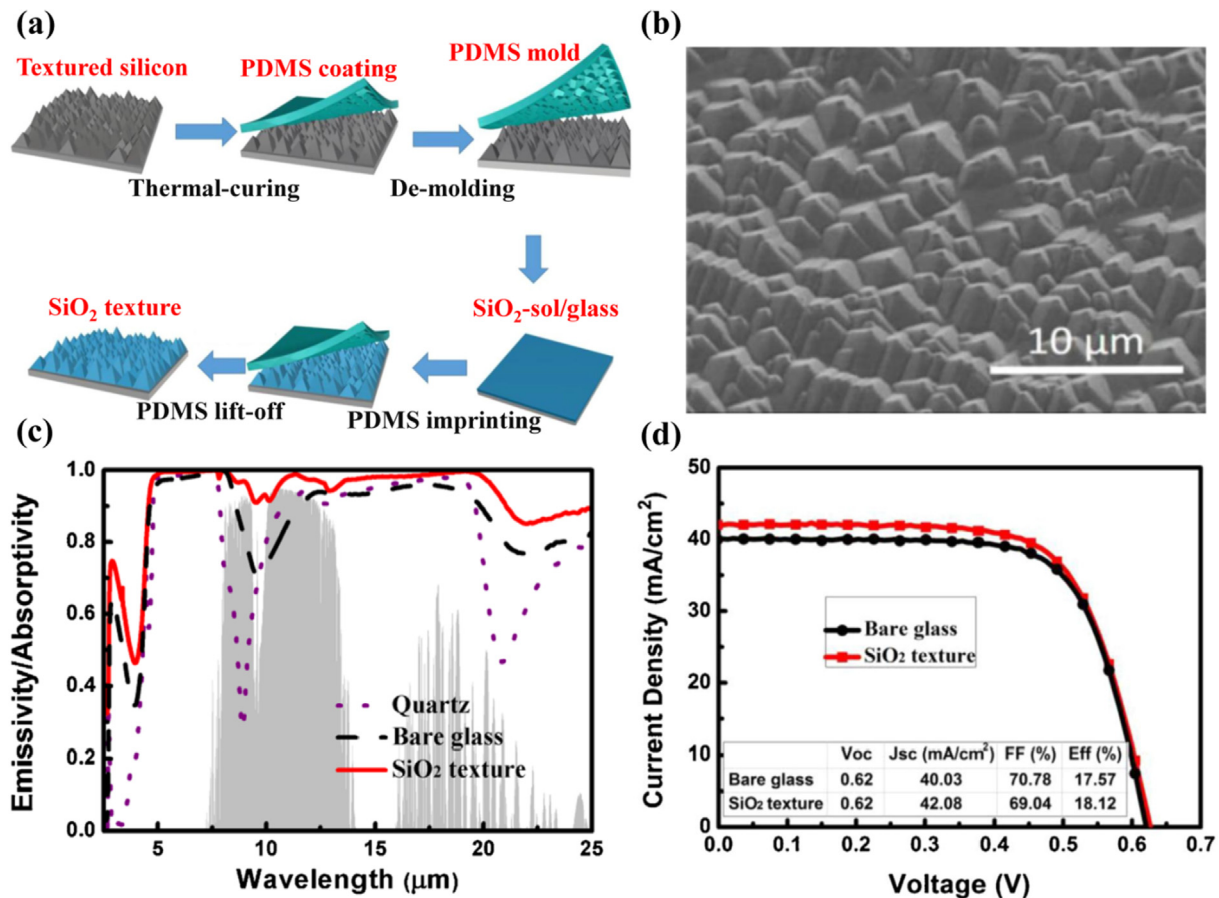
Fig. 27. Schematic of a universal routine to enhance the radiative cooling ability of silicon solar cell, as taken from Ref. [117]. (a) Schematic of universal routine. (b) SEM image of silica texture. (c) Spectral characterization of silica texture, with spectral properties of quartz and glass for reference. (d) I–V curves of the silica texture PV module and conventional glass-encapsulated PV module.

part of solar energy can be converted into electricity, whereas the remaining absorbed solar energy is dissipated into heat, increasing the operating temperature of solar cells. However, the PV efficiency is decreased by high temperature. For example, a 1 K temperature increase can reduce the relative efficiency by approximately 0.4–0.5% for a crystalline silicon solar cell. Thus, radiative cooling method is a good choice for passively cooling solar cells.

In current PV applications, the silicon solar cell is still the mainstream product. From the physical viewpoint, the infrared emissivity of bare silicon is small; indicating that self-cooling by radiative cooling is limited. A common approach to increase the effect of radiative cooling for cells is to apply a "transparent radiator" on top of solar cells. This "transparent radiator" should be highly transmitted for solar radiation and strongly emissive over the mid-infrared wavelength band. Zhu et al. proposed two typical "transparent radiators" (Fig. 26), including bulk silica with array of pyramid [20] and air holes [95], to enhance the radiative cooling of solar cells. The results show that the temperature reduction can reach 18.3 K and 13 K.

In a conventional PV module, a transparent cover, such as glass, is applied to the top of solar cells. The hemispherical emissivity for commercial glass is approximately 0.82–0.84, indicating that the strong radiative cooling ability already exists in a commercial PV module [138]. Under this condition, progress has been made to further enhance the radiative cooling ability for the PV module. Lu et al. [117] developed a universal routine to improve the radiative cooling ability of silicon solar cells by adding ultra-broadband versatile textures (Fig. 27) on the cells. The average emissivity of the modified solar cell within 8–13 μm is improved above 0.96 from spectral testing and the PV efficiency is also increased by 3.13% relative to the commercial glass

encapsulated PV module.

Apart from the silicon solar cell, other solar cells, such as gallium arsenide (GaAs) [139] and CIGS solar cell [140], can be passively cooled by radiative cooling. Moreover, radiative cooling methods can be used in extraterrestrial PV system [141], concentrating PV (CPV) system [142,143], and thermal PV (TPV) system [144]. Munday et al. [139,141] theoretically estimated the potential effect of radiative cooling on cooling GaAs solar cells based on the method of detailed balance (Fig. 28(a)). The results showed that the operating temperature of the solar cell can be reduced by 18 °C via radiative cooling approach, yielding an improvement in operating voltage of GaAs cell corresponding to PV conversion efficiency. Sun et al. [142] designed a special radiator that consists of low-iron soda-lime glass with a porous layer on top and developed a related radiative cooling method for the CPV system. A similar radiator was also proposed and applied to the TPV system (Fig. 28(b)) [144].

Recently, a new concept of passive cooling method coupled radiative cooling with solar radiation management (Fig. 29), which is a modification of the idea of "transparent radiator," was proposed for cooling solar cells. The radiation management is essentially the reflection of photons that cannot be used to generate electron–hole pairs, which can decrease the absorption of solar energy for solar cells and passively cool cells. Li et al. [22] designed a photonic radiator for the silicon-based PV module, which comprised a multilayer structure that exhibits strong thermal emission while also substantially reflecting the solar radiation within 1.1–4 μm and ultraviolet regimes. Simulation study reveals that the temperature of silicon cell can be reduced by 5.7 °C after applying the aforementioned radiator to a PV module. Furthermore, Sun et al. [140] numerically estimated the cooling
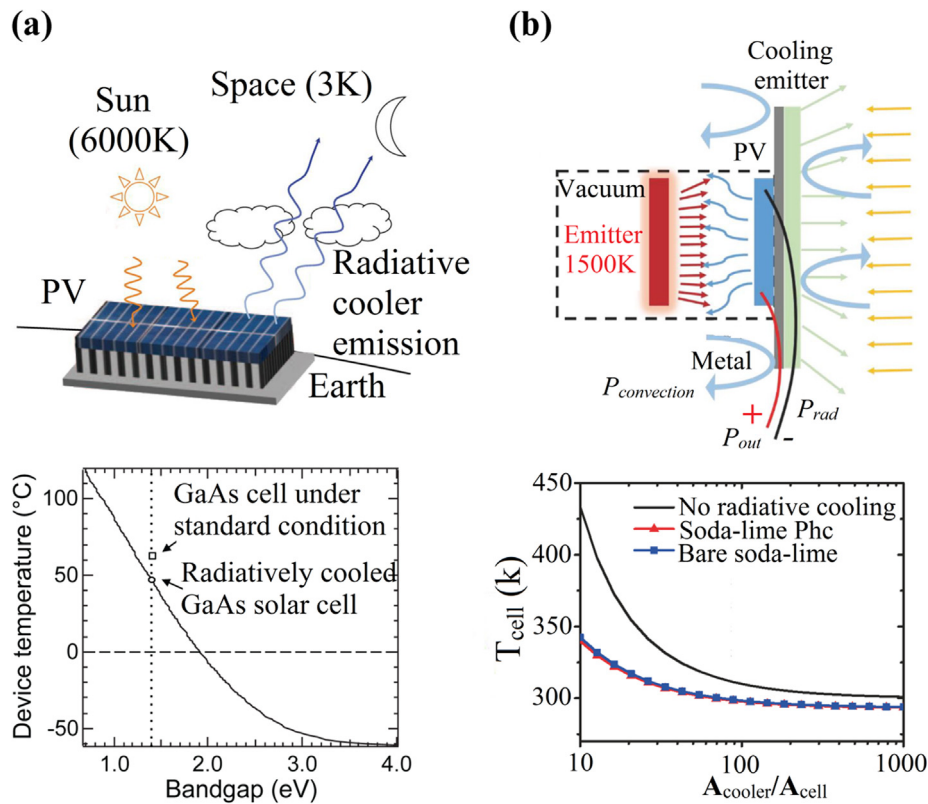
Fig. 28. Radiative cooling method for different solar cells and PV applications. (a) Schematic of radiative cooing for GaAs solar cells as reported in Ref. [139]. (b) Schematic of radiative cooling for TPV system as reported in Ref. [144].
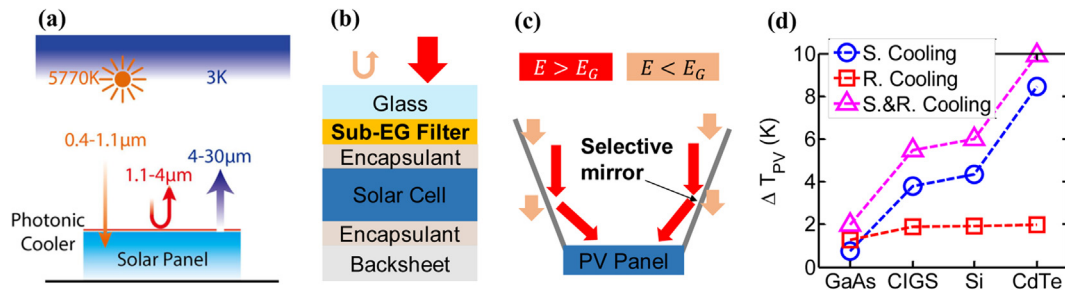

Fig. 29. New concept of passive cooling method coupled radiative cooling with solar radiation management for PV cooling. (a) Schematic of new cooling method for silicon PV module, as taken from Ref. [22]. (b)–(d) Possible implementations of new cooling approach and its potential for cooling different cells, as taken from Ref. [140].

potential of integration of radiative cooling and management, which show that the temperature of solar cells can be reduced up to 10 °C and 20 °C for one-sun and low-concentration photovoltaic systems, respectively.

4.3. Personal thermal management

Personal thermal management by passive radiative cooling and heating is an emerging topic in the engineering field and has huge potential to considerably reduce fossil energy consumption. Human skin has been proven to be a near-black radiator with an emissivity over 0.95 [145,146] for all levels of physical activity, such as perspiration. Therefore, properly controlling the thermal radiation energy of skin is a feasible approach to passively manage the thermal comfort of humans. Currently, clothing outside the skin is the main subject of research. First, the cloth must be opaque for visible light due to the considerations of actual application and prevention of sunlight absorption. Second, if the cloth is transparent for thermal radiation of the skin, then

humans will be radiatively cooled; otherwise, humans will be radiatively heated. Indicating that this mechanism is essentially the control of the aforementioned conventional radiative cooling is necessary; however, the cold source is not only the universe and will be constantly changing.

The cloth should be transparent to mid-infrared thermal radiation and opaque-to-visible sunlight (ITVO) to fully dissipate thermal radiation from the human body. Tong et al. [146] proposed a model of ITVO fabric (ITVOF) for personal radiative cooling based on thermal and optical simulations. Moreover, a sample of ITVOF was fabricated via an optimized integration of synthetic polymer fibers with a low-infrared absorptance. A similar concept was also investigated by Cui et al. [147–149]. Hsu et al. [147] proved that nanoporous polyethylene (nanoPE) is one of the ITVO materials due to its pore size distribution. Then, an ITVO textile (ITVOT) was structured and fabricated based on nanoPE material. The experimental comparison demonstrated that the skin temperature can be cooled by 2.0 °C when covered with the ITVOT to replace traditional cotton. Furthermore, an approach for large-scale
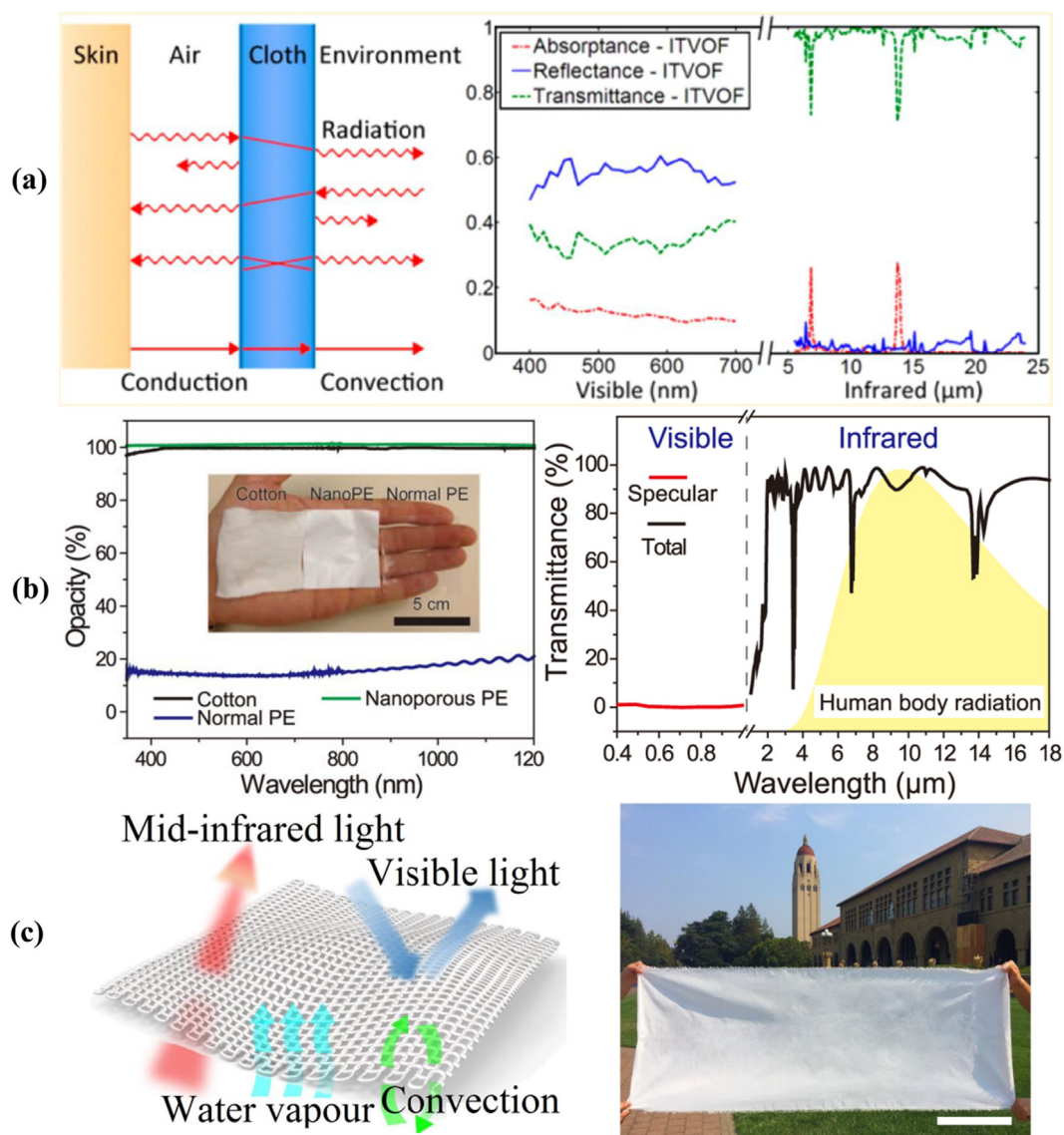
Fig. 30. Enhanced radiative cooling for passive cooling of human body. (a) Schematic of heat balance among skin, cloth, and environment and spectral characterization of ITVOF taken from Ref. [146]. (b) Photo and spectral characterization of nanoPE taken from Ref. [147]. (c) Schematic of the nanoPE fabic and photo of a large woven nanoPE fabic from Ref. [148].

ITVOT was developed based on the nanoPE microfibers [148]. The related schematics are presented in Fig. 30.

By contrast, if passive radiative heating is needed, then the spectral property of cloth should be designed to decrease the effect of radiative cooling from the human body to the cloth and the environment. To meet such a demand, the inner surface of the cloth should be highly reflective of thermal radiation and the outside surface of the cloth should have low emission. Cai et al. [150] designed a novel textile (Fig. 31(a)) based on nanoporous metalized polyethylene to meet the spectral selective demand for passive heating, which can enable more than 7 °C skin temperature reduction compared with that of normal textile. Based on the contribution of single-mode radiative cooling and heating, a dual-mode textile (Fig. 31(b)) combining radiative cooling and heating for the human body was proposed and developed by Hsu et al. [151] via a bilayer radiator embedded inside a nanoPE layer.

4.4. Other potential applications

In this part, several potential applications of radiative cooling were introduced and analyzed, which will be an essential reference for application development of radiative cooling in the future.

First, obtaining an ultra-low temperature phenomenon in terrestrial environment is possible by radiative cooling. According to the cooling principle of radiative cooling (Section 2.5), the equilibrium temperature of a narrowband-ideal radiator can reach approximately 200 K by decreasing the effect of intrinsic cooling loss on the cooling performance of the radiator. Thus, achieving an ultra-low temperature by radiative cooling in terrestrial environment is possible and can be a crucial opportunity for industry applications, such as medicine and chemical research and deep-sea fishing. On this topic, Chen et al. [45] experimentally demonstrated a temperature reduction of 37 °C from ambient surrounding temperature via an entire day–night cycle, with a maximum temperature reduction of 42 °C. The key contribution of this experiment is that the selective radiator was designed to be thermally decoupled with the atmosphere and sun while simultaneously maintaining coupling to the universe by sun shade and ZnSe window (Fig. 32). ZnSe window is a hard cover, which is different from a flexible film-based shield reported in almost all previous studies. The vacuum environment for the radiator can be realized only through this approach.
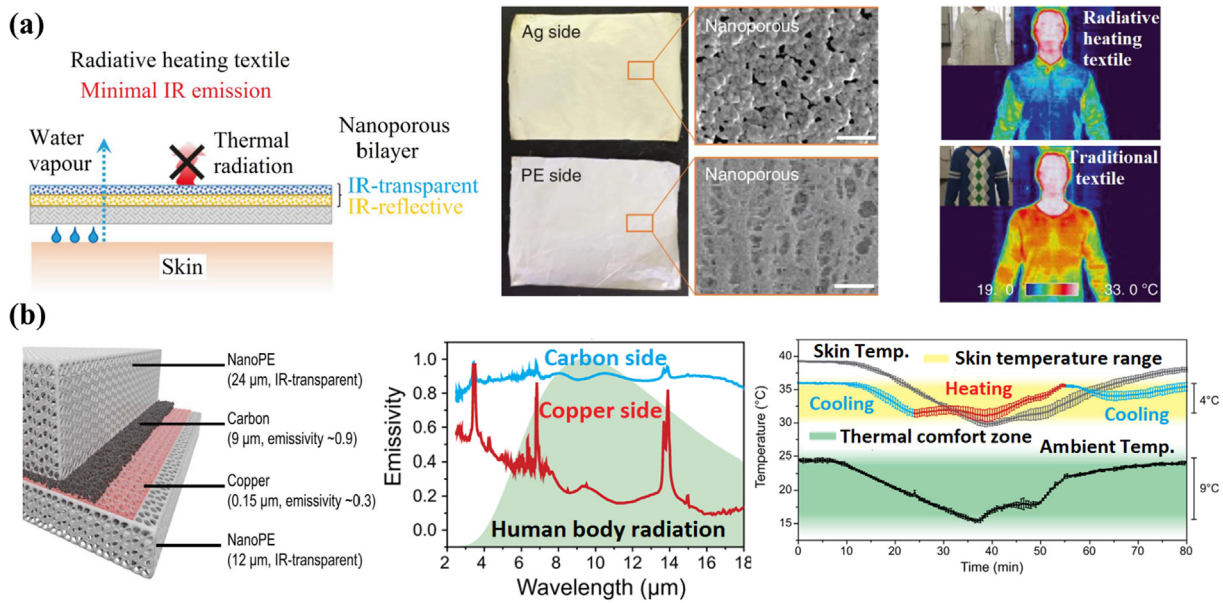
Fig. 31. (a) Schematic of a novel textile based on nanoporous metallized polyethylene and thermal imaging and photos of human body wearing novel and traditional textile taken from Ref. [150]. (b) Schematic, spectral characterization, and performance evaluation of a dual-mode textile taken from Ref. [151].
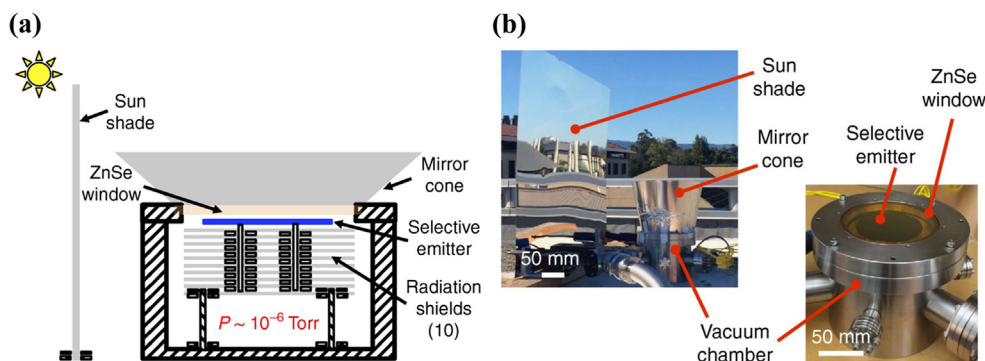

Fig. 32. Experimental demonstration of ultra-low temperature by radiative cooling [45].

Second, maintaining thermal homeostasis using radiative cooling via phase-change material (PCM) is also an interesting potential application. Vanadium dioxide (VO₂), a novel PCM, exhibits a dramatic change in optical properties near its phase-change temperature, which is a good feature for switchable thermal emission. Wu et al. [152] designed VO₂-coated silicon micro-cones for thermal homeostasis (Fig. 33(a)). When the surface temperature is lower than the phase-change temperature of VO₂ (corresponding to its insulating state), the emissivity of the structure is low; otherwise (corresponding to the metallic state of VO₂), the emissivity increases. Wu et al. [153] proposed a tunable mid-infrared metasurface, as shown in Fig. 33(b), for temperature control. The radiative cooling power of the metasurface can be switched fourfold as the surface temperature is below/above VO₂'s phase change temperature. Similar researches of PCM-based radiative cooling were conducted by Kort-Kamp [154] and Ono [155].

Third, harvesting renewable energy from thermal radiation is another potential topic in radiative cooling. Harvesting energy on the basis of energy flux flowing from the hot to the cold source is generally possible. According to the essence of radiative cooling, the cold source can be created by radiative cooling while the earth is the hot source. Thus, such an approach is an opportunity to harvest renewable energy from the earth's thermal radiation. Byrnes et al. [156] proposed a novel concept of the device (Fig. 34), namely, emissive energy harvester (EEH), based on the preceding consideration. Moreover, two EEH designs were developed: a thermal EEH and an optoelectronic EEH.

Considering the total thermal radiation from the earth to the universe, this concept will be an advanced technology to harvest renewable energy.

5. Conclusions

In summary, the current state of the art involved in passive radiative cooling technology is reviewed and updated on the basis of fundamental principles, advanced materials and radiators, and potential developments. Passive cooling is essentially the energy balance between the radiator and environment, involving the effects of thermal radiation, infrared sky radiation, solar radiation, and parasitic cooling loss. Nocturnal radiative cooling with infrared black and/or infrared selective radiators was the main topic in previous studies. With the current progress in nano-/micro-photonic radiator and metamaterials, diurnal radiative cooling has been demonstrated in recent years. Furthermore, passive radiative cooling can be applied in various applications, including energy-efficient buildings, photovoltaic cooling, and personal thermal management. Thus, passive radiative cooling will still be a research hotspot to achieve further developments. In addition, several recommendations for further investigation are presented in the following:

- For sub-ambient applications, the topic of hard cover with high transmittance within the atmospheric window should be further
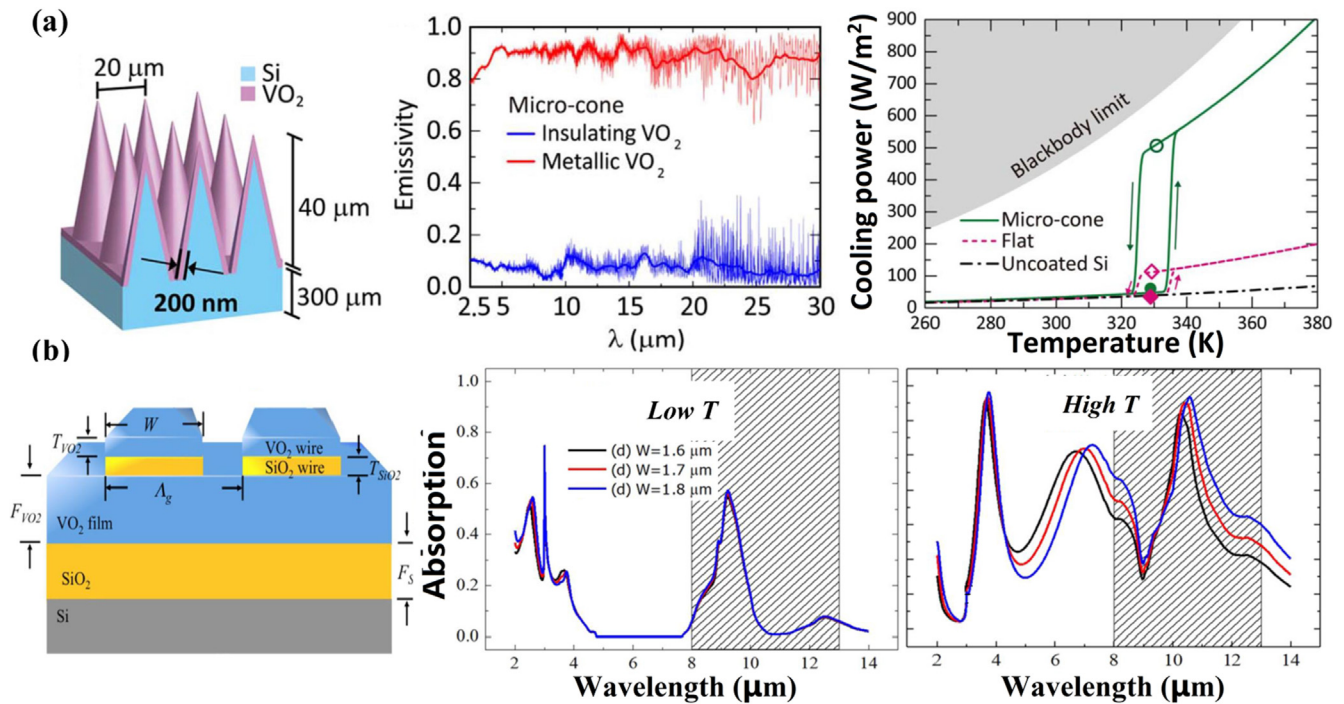
Fig. 33. Radiative cooling for thermal homeostasis via PCM-based structure. (a) VO$_2$-coated silicon micro-cones taken from Ref. [152]. (b) PCM-based metasurface that consists of SiO$_2$ and VO$_2$ taken from Ref. [153].
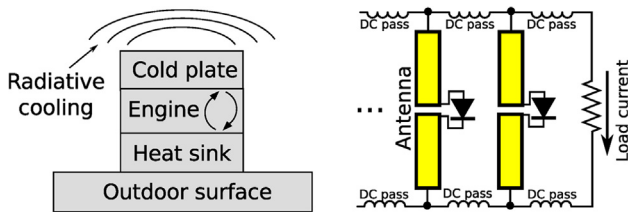

Fig. 34. Schematic of EEH. The left EEH is a thermal EEH, while the right EEH is an infrared rectenna EEH [156].

investigated. At present, flexible thin films, such as low-density polyethylene film, are the main choice for research investigation, which is unreliable for real applications. Moreover, if the cover is hard, then parasitic cooling loss of the cooling system will be largely decreased by the vacuum environment, which will be a major revolution for radiative cooling technology.

- For diurnal radiative cooling, although some metamaterials were developed to decrease the cost and scale of the radiator, the design and fabrication of large-scale cost-efficient radiators remain a major challenge for commercial application.
- The seasonal and/or regional applicability of radiative cooling should be further evaluated, especially for diurnal radiative cooling. The effect of sky condition, a comprehensive integration of geography, climatic condition, and et al., is a vital parameter for radiative cooling. Thus, the investigation of seasonal and/or regional applicability for radiative cooling will be an important reference for its applications.
- The efficient conversion of cooling energy for radiative cooling is a good topic for further exploration. Cold storage, such as PCM cold storage, has been regarded in recent studies as one of the efficient ways of cooling utilization. Apart from cold storage, other efficient ways should be developed.
- The stability and durability of different radiators, especially for polymer related radiators should be systematically investigated and compared, which will be an essential reference for application of radiative cooling.

References

[1] Modest MF. Radiative heat transfer. 2nd ed. Academic press; 2003.
[2] Zhang Z. Nano/Microscale heat transfer. New York: McGraw-Hill; 2007.
[3] Gerald M, Tebaldi C. More intense, more frequent, and longer lasting heat waves in the 21st century. Science (80-) 2004;305:994–7.
[4] Bliss RW. Atmospheric radiation near the surface of the ground: a summary for engineers. Sol Energy 1961;5:103–20.
[5] Zevenhoven R, Fält M. Radiative cooling through the atmospheric window: a third, less intrusive geoengineering approach. Energy 2018;152:27–33.
[6] Catalanotti S, Cuomo V, Piro G, Ruggi D, Silvestrini V, Troise G. The radiative cooling of selective surfaces. Sol Energy 1975;17:83–9.
[7] Hossain MM, Gu M. Radiative cooling: principles, progress, and potentials. Adv Sci 2016;3:1500360.
[8] Kimball BA, Idso SB, Aase JK. A model of thermal radiation from partly cloudy and overcast skies. Water Resour Res 1982;18:931–6.
[9] Sugita M, Brutsaert W. Cloud effect in the estimation of instantaneous downard longwave radiation. Water Resour Res 1993;29:599–605.
[10] Khedari J, Waewsak J, Thepa S, Hirunlabh J. Field investigation of night radiation cooling under tropical climate. Renew Energy 2000;20:183–93.
[11] Tso CY, Chan KC, Chao CYH. A field investigation of passive radiative cooling under Hong Kong's climate. Renew Energy 2017;106:52–61.
[12] Zeyghami M, Goswami DY, Stefanakos E. A review of clear sky radiative cooling developments and applications in renewable power systems and passive building cooling. Sol Energy Mater Sol Cells 2018;178:115–28.
[13] Raman AP, Anoma MA, Zhu L, Rephaeli E, Fan S. Passive radiative cooling below ambient air temperature under direct sunlight. Nature 2014;515:540–4.
[14] Family R, Mengüç MP. Materials for radiative cooling: a review. Proc Environ Sci 2017;38:752–9.
[15] Lu X, Xu P, Wang H, Yang T, Hou J. Cooling potential and applications prospects of passive radiative cooling in buildings: the current state-of-the-art. Renew Sustain Energy Rev 2016;65:1079–97.
[16] Sun X, Sun Y, Zhou Z, Alam MA, Bermel P. Radiative sky cooling: fundamental physics, materials, structures, and applications. Nanophotonics 2017;6:997–1015.
[17] Vall S, Castell A. Radiative cooling as low-grade energy source: a literature review. Renew Sustain Energy Rev 2017;77:803–20.
[18] Bergman TL, Lavine AS, Incropera FP, DeWitt DP. Fundamentals of heat and mass

transfer. 7th ed. John Wiley & Sons; 2011.

[19] Granqvist CG, Hjortsberg A. Radiative cooling to low temperatures: general considerations and application to selectively emitting SiO films. J Appl Phys 1981;52:4205–20.

[20] Zhu L, Raman A, Wang KX, Anoma MA, Fan S. Radiative cooling of solar cells. Optica 2014;1:32–8.

[21] Bao H, Yan C, Wang B, Fang X, Zhao CY, Ruan X. Double-layer nanoparticle-based coatings for efficient terrestrial radiative cooling. Sol Energy Mater Sol Cells 2017;168:78–84.

[22] Li W, Shi Y, Chen K, Zhu L, Fan S. A comprehensive photonic approach for solar cell cooling. ACS Photon 2017;4:774–82.

[23] Lushiku EM, Hjortsberg A, Granqvist CG. Radiative cooling with selectively infrared-emitting ammonia gas. J Appl Phys 1982;53:5526–30.

[24] Lushiku EM, Granqvist C-G. Rative cooling with selectively infrared-emitting gases. Appl Opt 1984;23:1835–43.

[25] Berdahl P, Martin M, Sakkal F. Thermal performance of radiative cooling panels. Int J Heat Mass Transf 1983;26:871–80.

[26] Castro Aguilar JL, Gentle AR, Smith GB, Chen D. A method to measure total atmospheric long-wave down-welling radiation using a low cost infrared thermometer tilted to the vertical. Energy 2015;81:233–44.

[27] Brunt D. Notes on radiation in the atmosphere. I. Q J R Meteorol Soc 1932;58:389–420.

[28] Angström AK. Effective radiation during the second international polar year. Medde Stat Met Hydrogr Anst 1936.

[29] Swinbank WC. Longwave radiation from clear sky. Q J R Meteorol Soc 1963;89:339–48.

[30] Idso SB, Jackson RD. Thermal radiation from the atmosphere. J Geophys Res 1969;74:5397–403.

[31] Staley DO, Jurica GM. Effective atmospheric emissivity under clear skies. J Appl Meteorol 1972;11:349–56.

[32] Skies FC. A set of equations for full spectrum and 8- to 14-μm and 10.5- to 12.5-μm thermal radiation from cloudless skies. Water Resour 1981;17:295–304.

[33] Berdahl P, Fromberg R. The thermal radiance of clear skies. Sol Energy 1982;29:299–314.

[34] Berdahl P, Martin M. Emissivity of clear skies. Sol Energy 1984;32:663–4.

[35] Berger X, Buriot D, Garnier F. About the equivalent radiative temperature for clear skies. Sol Energy 1984;32:725–33.

[36] Martin M, Berdahl P. Characteristics of infrared sky radiation in the United States. Sol Energy 1984;33:321–36.

[37] Chen B, Maloney J, Clark D, Mei WN. Measurement of night sky emissivity in determining radiant cooling from cool storage roofs and roof ponds. Proc Natl Passiv Sol Conf 1995;20:310–3.

[38] Niemelä S, Räisänen P, Savijärvi H. Comparison of surface radiative flux parameterizations part I: longwave radiation. Atmos Res 2001;58:1–18.

[39] Tang R, Etzion Y, Meir IA. Estimates of clear night sky emissivity in the Negev Highlands, Israel. Energy Convers Manag 2004;45:1831–43.

[40] Lhomme JP, Vacher JJ, Rocheteau A. Estimating downward long-wave radiation on the Andean Altiplano. Agric For Meteorol 2007;145:139–48.

[41] Sicart JE, Hock R, Ribstein P, Chazarin JP. Sky longwave radiation on tropical Andean glaciers: parameterization and sensitivity to atmospheric variables. J Glaciol 2010;56:854–60.

[42] Das AK, Iqbal M. A simplified technique to compute spectral atmospheric radiation. Sol Energy 1987;39:143–55.

[43] Iqbal M, editor. An introduction to solar radiation. Academic press; 1983.

[44] Zhao B, Hu M, Ao X, Pei G. Conceptual development of a building-integrated photovoltaic–radiative cooling system and preliminary performance analysis in Eastern China. Appl Energy 2017;205:626–34.

[45] Chen Z, Zhu L, Raman A, Fan S. Radiative cooling to deep sub-freezing temperatures through a 24-h day-night cycle. Nat Commun 2016;7:13729.

[46] Hu M, Zhao B, Li J, Wang Y, Pei G. Preliminary thermal analysis of a combined photovoltaic–photothermic–nocturnal radiative cooling system. Energy 2017;137:419–30.

[47] Nilsson NA, Eriksson TS, Granqvist CG. Infrared-transparent convection shields for radiative cooling: initial results on corrugated polyethylene foils. Sol Energy Mater 1985;12:327–33.

[48] Nilsson TMJ, Niklasson GA, Granqvist CG. A solar reflecting material for radiative cooling applications: ZnS pigmented polyethylene. Sol Energy Mater Sol Cells 1992;28:175–93.

[49] Nilsson TMJ, Niklasson GA. Radiative cooling during the day: simulations and experiments on pigmented polyethylene cover foils. Sol Energy Mater Sol Cells 1995;37:93–118.

[50] Golaka A, Exell RHB. An investigation into the use of a wind shield to reduce the convective heat flux to a nocturnal radiative cooling surface. Renew Energy 2007;32:593–608.

[51] Chow TT. Performance analysis of photovoltaic-thermal collector by explicit dynamic model. Sol Energy 2003;75:143–52.

[52] Kou J Long, Jurado Z, Chen Z, Fan S, Minnich AJ. Daytime radiative cooling using near-black infrared emitters. ACS Photon 2017;4:626–30.

[53] IR Transmission Spectra; 2018. < http://www.gemini.edu/sciops/telescopes-and-sites/observing-condition-constraints/ir-transmission-spectra > [accessed February 21, 2018].

[54] Orel B, Gunde MK, Krainer A. Radiative cooling efficiency of white pigmented paints. Sol Energy 1993;50:477–82.

[55] Granqvist CG. Radiative heating and cooling with spectrally selective surfaces. Appl Opt 1981;20:2606–15.

[56] Granqvist CG, Hjortsberg A. Surfaces for radiative cooling: silicon monoxide films on aluminum. Appl Phys Lett 1980;36:139–41.

[57] Granqvist CG, Hjortsberg A, Eriksson TS. Radiative cooling to low temperatures with selectivity IR-emitting surfaces. Thin Solid Films 1982;90:187–90.

[58] Huang Z, Ruan X. Nanoparticle embedded double-layer coating for daytime radiative cooling. Int J Heat Mass Transf 2017;104:890–6.

[59] Zhai Y, Ma Y, David SN, Zhao D, Lou R, Tan G, et al. Scalable-manufactured randomized glass-polymer hybrid metamaterial for daytime radiative cooling. Science (80-) 2017;355:1062–6.

[60] Curtis OF. Leaf temperatures and the cooling of leaves by radiation. Plant Physiol 1936;11:343.

[61] Matsui T, Eguchi H, Mori K. Control of dew and frost formations on leaf by radiative cooling. Environ Control Biol 1981;19:51–7.

[62] Okada M, Okada M, Kusaka H. Dependence of atmospheric cooling by vegetation on canopy surface area during radiative cooling at night: physical model evaluation using a polyethylene chamber. J Agric Meteorol 2016;72:20–8.

[63] Shi NN, Tsai C-C, Camino F, Bernard GD, Yu N, Wehner R. Keeping cool: enhanced optical reflection and radiative heat dissipation in Saharan silver ants. Science (80-) 2015;349:298–301.

[64] Bartoli B, Catalanotti S, Coluzzi B, Cuomo V, Silvestrini V, Troise G. Nocturnal and diurnal performances of selective radiators. Appl Energy 1977;3:267–86.

[65] Addeo A, Monza E, Peraldo M, Bartoli B, Coluzzi B, Silvestrini V, et al. Selective covers for natural cooling devices. Nuovo Cim C 1978;1:419–29.

[66] Trombe F. Perspectives sur l'utilisation des rayonnements solaires et terrestres dans certaines régions du monde. Rev Gen Therm 1967;6:1285.

[67] Grenier P. Réfrigération radiative. Effet de serre inverse. Rev Phys Appl 1979;14:87–90.

[68] Landro B, McCormick PG. Effect of surface characteristics and atmospheric conditions on radiative heat loss to a clear sky. Int J Heat Mass Transf 1980;23:613–20.

[69] Bartoli B, Coluzzi B, Silvestrini V, Addeo A, Nicolais L, Romero G. Light selective structures for large scale natural air conditioning. Sol Energy 1980;24:93–8.

[70] Czapla B. Potential for passive radiative cooling by PDMS selective emitters. Proc ASME 2017 Heat Transf Summer Conf 2017.

[71] Hu M, Pei G, Wang Q, Li J, Wang Y, Ji J. Field test and preliminary analysis of a combined diurnal solar heating and nocturnal radiative cooling system. Appl Energy 2016;179:899–908.

[72] Harrison AW, Walton MR. Radiative cooling of TiO2 white paint. Sol Energy 1978;20:185–8.

[73] Michell D, Biggs KL. Radiation cooling of buildings at night. Appl Energy 1979;5:263–75.

[74] Hjortsberg A, Granqvist CG. Infrared optical properties of silicon monoxide films. Appl Opt 1980;19:1694–6.

[75] Eriksson TS, Granqvist CG. Infrared optical properties of electron-beam evaporated silicon oxynitride films. Appl Opt 1983;22:3204–6.

[76] Eriksson TS, Lushiku EM, Granqvist CG. Materials for radiative cooling to low temperature. Sol Energy Mater 1984;11:149–61.

[77] Eriksson TS, Jiang SJ, Granqvist CG. Surface coatings for radiative cooling applications: Silicon dioxide and silicon nitride made by reactive RF-sputtering. Sol Energy Mater 1985;12:319–25.

[78] Palik ED. Handbook of optical constants of solids. Academic press; 1985.

[79] Berdahl P. Radiative cooling with MgO and/or LiF layers. Appl Opt 1984;23:370–2.

[80] Gentle AR, Smith GB. Radiative heat pumping from the Earth using surface phonon resonant nanoparticles. Nano Lett 2010;10:373–9.

[81] Zhang X. Metamaterials for perpetual cooling at large scales. Science (80-) 2017;355:1023–4.

[82] Li W, Fan S. Nanophotonic control of thermal radiation for energy applications [Invited]. Opt Express 2018;26:15995–6021.

[83] Kecebas MA, Menguc MP, Kosar A, Sendur K. Passive radiative cooling design with broadband optical thin-film filters. J Quant Spectrosc Radiat Transf 2017;198:179–86.

[84] Gentle AR, Smith GB. A subambient open roof surface under the mid-summer sun. Adv Sci 2015;2:1500119.

[85] Huang Y, Pu M, Zhao Z, Li X, Ma X, Luo X. Broadband metamaterial as an "invisible" radiative cooling coat. Opt Commun 2018;407:204–7.

[86] Tikhonravov AV, Trubetskov MK, DeBell GW. Application of the needle optimization technique to the design of optical coatings. Appl Opt 1996;35:5493–508.

[87] Tikhonravov AV, Trubetskov MK, DeBell GW. Optical coating design approaches based on the needle optimization technique. Appl Opt 2007;46:704–10.

[88] Boudet T, Chaton P, Herault L, Gonon G, Jouanet L, Keller P. Thin-film designs by simulated annealing. Appl Opt 1996;35:6219–26.

[89] Li L, Wang Q-H, Li D-H, Peng H-R. Jump method for optical thin film design. Opt Express 2009;17:16920–6.

[90] Shi Y, Li W, Raman A, Fan S. Optimization of multilayer optical films with a memetic algorithm and mixed integer programming. ACS Photon 2018;5:684–91.

[91] TFCala; 2018. < http://www.sspectra.com/ > [accessed June 2, 2018].

[92] THIN FILM CENTER: Essential Macleod; 2018. < https://www.thinfilmcenter.com/essential.php > [accessed June 2, 2018].

[93] Zhu L, Raman A, Fan S. Color-preserving daytime radiative cooling. Appl Phys Lett 2013;103:223902.

[94] Li W, Shi Y, Chen Z, Fan S. Photonic thermal management of coloured objects. Nat Commun 2018;9:4240.

[95] Zhu L, Raman AP, Fan S. Radiative cooling of solar absorbers using a visibly transparent photonic crystal thermal blackbody. Proc Natl Acad Sci 2015;112:12282–7.

[96] Wu D, Liu C, Xu Z, Liu Y, Yu Z, Yu L, et al. The design of ultra-broadband selective

near-perfect absorber based on photonic structures to achieve near-ideal daytime radiative cooling. Mater Des 2018;139:104–11.

[97] Rephaeli E, Raman A, Fan S. Ultrabroadband photonic structures to achieve high-performance daytime radiative cooling. Nano Lett 2013;13:1457–61.

[98] Hossain MM, Jia B, Gu M. A metamaterial emitter for highly efficient radiative cooling. Adv Opt Mater 2015;3:1047–51.

[99] Johnson TE. Radiation cooling of structures with infrared transparent wind screens. Sol Energy 1975;17:173–8.

[100] Hjortsberg A, Granqvist CG. Radiative cooling with selectively emitting ethylene gas. Appl Phys Lett 1981;39:507–9.

[101] Lushiku EM, Eriksson TS, Hjortsberg A, Granqvist CG. Radiative cooling to low temperatures with selectively infrared-emitting gases. Sol Wind Technol 1984;1:115–21.

[102] Dan Phuong Dung, Chinnappa JCV. The cooling of water flowing over an inclined surface exposed to the night sky. Sol Wind Technol 1989;6:41–50.

[103] Etzion Y, Erell E. Low-cost long-wave radiators for passive cooling of buildings. Archit Sci Rev 1999;42:79–85.

[104] Ito S, Miura N. Studies of radiative cooling systems for storing thermal energy. ASME J Sol Energy Eng 1989;111:251–6.

[105] Hamza A, Taha IMS, Ismail IM. Cooling of water flowing through a night sky radiator. Sol Energy 1995;55:235–53.

[106] Ezekwe CI. Nocturnal radiation measurements in Nigeria. Sol Energy 1986;37:1–6.

[107] Ezekwe CI. Performance of a heat pipe assisted night sky radiative cooler. Energy Convers Manag 1990;30:403–8.

[108] Diatezua MD, Thiry PA, Caudano R. Characterization of silicon oxynitride multi-layered systems for passive radiative cooling application. Vacuum 1995;46:1121–4.

[109] Tazawa M, Jin P, Tanemura S. Thin film used to obtain a constant temperature lower than the ambient. Thin Solid Films 1996;281:232–4.

[110] Tazawa M, Jin P, Yoshimura K, Miki T, Tanemura S. New material design with V1−xWxO2 film for sky radiator to obtain temperature stability. Sol Energy 1998;64:3–7.

[111] Miyazaki H, Okada K, Jinno K, Ota T. Fabrication of radiative cooling devices using Si2N2O nano-particles. J Ceram Soc Japan 2016;124:1185–7.

[112] Zou C, Ren G, Hossain MM, Nirantar S, Withayachumnankul W, Ahmed T, et al. Metal-loaded dielectric resonator metasurfaces for radiative cooling. Adv Opt Mater 2017;5:1700460.

[113] Suichi T, Ishikawa A, Hayashi Y, Tsuruta K. Structure optimization of metallodi-electric multilayer for high-efficiency daytime radiative cooling. Therm Radiat Manag Energy Appl 2017.

[114] Wu JY, Gong YZ, Huang PR, Ma GJ, Dai QF. Diurnal cooling for continuous thermal sources under direct subtropical sunlight produced by quasi-Cantor structure. Chinese Phys B 2017;26:104201.

[115] Atiganyanun S, Plumley JB, Han SJ, Hsu K, Cytrynbaum J, Peng TL, et al. Effective radiative cooling by paint-format microsphere-based photonic random media. ACS Photon 2018;5:1181–7.

[116] Mandal J, Fu Y, Overvig AC, Jia M, Sun K, Shi NN, et al. Hierarchically porous polymer coatings for highly efficient passive daytime radiative cooling. Science (80-) 2018;362:315–9.

[117] Lu Y, Chen Z, Ai L, Zhang X, Zhang J, Li J, et al. A universal route to realize radiative cooling and light management in photovoltaic modules. Sol RRL 2017;1:1700084.

[118] Sun K, Riedel CA, Wang Y, Urbani A, Simeoni M, Mengali S, et al. Metasurface optical solar reflectors using AZO transparent conducting oxides for radiative cooling of spacecraft. ACS Photon 2018;5:495–501.

[119] Omer AM. Energy, environment and sustainable development. Renew Sustain Energy Rev 2008;12:2265–300.

[120] Nwaigwe KN, Okoronkwo CA, Ogueke NV, Anyanwu EE. Review of nocturnal cooling systems. Int J Energy a Clean Environ 2010;11:117–43.

[121] Pearlmutter D, Berliner P. Experiments with a 'psychrometric' roof pond system for passive cooling in hot-arid regions. Energy Build 2017;144:295–302.

[122] Hosseinzadeh E, Taherian H. An experimental and analytical study of a radiative cooling system with unglazed flat plate collectors. Int J Green Energy 2012;9:766–79.

[123] Farmahini Farahani M, Heidarinejad G, Delfani S. A two-stage system of nocturnal radiative and indirect evaporative cooling for conditions in Tehran. Energy Build 2010;42:2131–8.

[124] Farmahini-Farahani M, Heidarinejad G. Increasing effectiveness of evaporative cooling by pre-cooling using nocturnally stored water. Appl Therm Eng 2012;38:117–23.

[125] Heidarinejad G, Farmahini Farahani M, Delfani S. Investigation of a hybrid system of nocturnal radiative cooling and direct evaporative cooling. Build Environ 2010;45:1521–8.

[126] Man Y, Yang H, Spitler JD, Fang Z. Feasibility study on novel hybrid ground coupled heat pump system with nocturnal cooling radiator for cooling load dominated buildings. Appl Energy 2011;88:4160–71.

[127] Zhao B, Hu M, Ao X, Xuan Q, Pei G. Comprehensive photonic approach for diurnal and nocturnal radiative cooling. Sol Energy Mater Sol Cells 2018;178:266–72.

[128] Hu M, Zhao B, Ao X, Su Y, Wang Y, Pei G. Comparative analysis of different surfaces for integrated solar heating and radiative cooling: a numerical study. Energy 2018;155:360–9.

[129] Eicker U, Dalibard A. Photovoltaic-thermal collectors for night radiative cooling of buildings. Sol Energy 2011;85:1322–35.

[130] Hu M, Pei G, Li L, Zheng R, Li J, Ji J. Theoretical and experimental study of spectral selectivity surface for both solar heating and radiative cooling. Int J Photoenergy 2015;2015..

[131] Fiorentini M, Cooper P, Ma Z. Development and optimization of an innovative HVAC system with integrated PVT and PCM thermal storage for a net-zero energy retrofitted house. Energy Build 2015;94:21–32.

[132] Hu M, Zhao B, Ao X, Zhao P, Su Y, Pei G. Field investigation of a hybrid photo-voltaic-photothermic-radiative cooling system. Appl Energy 2018;231:288–300.

[133] Zhang K, Zhao D, Yin X, Yang R, Tan G. Energy saving and economic analysis of a new hybrid radiative cooling system for single-family houses in the USA. Appl Energy 2018;224:371–81.

[134] Wang W, Fernandez N, Katipamula S, Alvine K. Performance assessment of a photonic radiative cooling system for office buildings. Renew Energy 2018;118:265–77.

[135] Goldstein EA, Raman AP, Fan S. Sub-ambient non-evaporative fluid cooling with the sky. Nat Energy 2017;2:17143.

[136] Smith G, Gentle A. Radiative cooling: energy savings from the sky. Nat Energy 2017;2:17142.

[137] Shockley W, Queisser HJ. Detailed balance limit of efficiency of p-n junction solar cells. J Appl Phys 1961;32:510–9.

[138] Gentle AR, Smith GB. Is enhanced radiative cooling of solar cell modules worth pursuing? Sol Energy Mater Sol Cells 2016;150:39–42.

[139] Munday JN, Safi T. Radiative cooling of a GaAs solar cell to improve power conversion efficiency. Photovolt Spec Conf (PVSC), 2016 IEEE 43rd 2016;1125–7.

[140] Sun X, Silverman TJ, Zhou Z, Khan MR, Bermel P, Alam MA. An optics-based approach to thermal management of photovoltaics: selective-spectral and radia-tive cooling. IEEE J Photovoltaics 2017;7:566–74.

[141] Safi TS, Munday JN. Improving photovoltaic performance through radiative cooling in both terrestrial and extraterrestrial environments. Opt Express 2015;23:A1120–8.

[142] Zhou Z, Sun Y, Sun X, Alam MA, Bermel P, Jin X. Radiative cooling for con-centrating photovoltaic systems. Therm Radiat Manag Energy Appl 2017.

[143] Nishioka K, Ota Y, Tamura K, Araki K. Heat reduction of concentrator photovoltaic module using high radiation coating. Surf Coat Technol 2013;215:472–5.

[144] Zhou Z, Sun X, Bermel P. Radiative cooling for thermophotovoltaic systems. Infrared Rem Sens Instrum 2016.

[145] Sanchez-Marin FJ, Calixto-Carrera S, Villaseñor-Mora C. Novel approach to assess the emissivity of the human skin. J Biomed Opt 2009;14:024006.

[146] Tong JK, Huang X, Boriskina SV, Loomis J, Xu Y, Chen G. Infrared-transparent visible-opaque fabrics for wearable personal thermal management. ACS Photon 2015;2:769–78.

[147] Hsu PC, Song AY, Catrysse PB, Liu C, Peng Y, Xie J, et al. Radiative human body cooling by nanoporous polyethylene textile. Science (80-) 2016;353:1019–23.

[148] Peng Y, Chen J, Song AY, Catrysse PB, Hsu P-C, Cai L, et al. Nanoporous poly-ethylene microfibres for large-scale radiative cooling fabric. Nat Sustain 2018;1:105–12.

[149] Cai L, Song AY, Li W, Hsu P-C, Lin D, Catrysse PB, et al. Spectrally selective na-nocomposite textile for outdoor personal cooling. Adv Mater 2018;30:1802152.

[150] Cai L, Song AY, Wu P, Hsu PC, Peng Y, Chen J, et al. Warming up human body by nanoporous metallized polyethylene textile. Nat Commun 2017;8:496.

[151] Hsu P-C, Liu C, Song AY, Zhang Z, Peng Y, Xie J, et al. A dual-mode textile for human body radiative heating and cooling. Sci Adv 2017;3:e1700895.

[152] Wu S-H, Chen M, Barako MT, Jankovic V, Hon PWC, Sweatlock LA, et al. Thermal homeostasis using microstructured phase-change materials. Optica 2017;4:1390–6.

[153] Wu S, Lai K, Wang C. Passive temperature control based on a phase change me-tasurface. Sci Rep 2018;8:7684.

[154] Kort-Kamp WJM, Kramadhati S, Azad AK, Reiten MT, Dalvit DAR. Passive radia-tive "thermostat" enabled by phase-change photonic nanostructures. ACS Photon 2018.

[155] Ono M, Chen K, Li W, Fan S. Self-adaptive radiative cooling based on phase change materials. Opt Express 2018;26:A777–87.

[156] Byrnes SJ, Blanchard R, Capasso F. Harvesting renewable energy from Earth's mid-infrared emissions. Proc Natl Acad Sci 2014;111:3927–32.